Conference on Molecular and
Atomic Gas Beams
Charlottesville, Virginia
May 13-14, 1963





JULY 1963

DEPARTMENT OF ENGINEERING



# status report on development of a high-speed high-intensity molecular beam





ELDON L. KNUTH

REPORT NO. 63-30

UNIVERSITY OF CALIFORNIA, LOS ANGELES

Report No. 63-30
July 1963

# STATUS REPORT ON DEVELOPMENT OF A HIGH-SPEED HIGH-INTENSITY MOLECULAR BEAM

Eldon L. Knuth
Associate Professor and
Head of Molecular-Beam Laboratory

Department of Engineering
University of California
Los Angeles 24, California

## FOREWORD

This paper reviews the historical development and current status of the Molecular-Beam Laboratory, Department of Engineering, University of California at Los Angeles. In the writing of this paper, possible interests of the sponsoring agencies, the future investigators in this laboratory and the contemporary investigators in other laboratories have been kept in mind. A summary of this publication was presented at the Conference on Molecular and Atomic Gas Beams and Related Problems held at the University of Virginia, 13-14 May 1963.

Financial support for the development of this laboratory has been provided chiefly by National Science Foundation Grant G-9783; the salary of the principal investigator during summer 1962 was supplied by NASA Grant NsG 237-62; the turbo-pump development was sponsored by UCLA Grant 1804; whereas a part of the cost of supplies, equipment and facilities has been borne by the Department of Engineering, University of California at Los Angeles. Beginning early in 1963, financial support is provided chiefly by NSF Grant GP-534, a two-year grant.

Of the many contributions to the development of this laboratory, the author would like to single out, for explicit acknowledgement, the generous contributions of the eight graduate students (R. J. Henry, J. P. Callinan, R. L. Plue, G. L. Johnston, N. M. Kuluva, J. W. Barnes, Jr., S. F. Iacobellis and D. Quan) who have completed M.S. theses and two graduate students (S. S. Fisher and A. E. Goldstein) who expect to complete, in the near future, M.S. theses in this laboratory. The eight completed theses are referenced at appropriate points throughout this paper.

## ABSTRACT

Status of the high-speed high-intensity molecular beam being developed in the Department of Engineering, UCLA, is described. Bases for designs of the several components are presented.

Using an arc-heated source and a hypersonic jet, molecular energies exceeding 1 ev and beam intensities of the order of $10^{16}$ molecules/$cm^2$ sec are anticipated. A two-disk beam chopper and speed selector provides a means for analyzing the speed distribution in the generated beam, for chopping the beam into bursts of nearly monoenergetic molecules suitable for scattering studies using the time-of-flight technique, and for modulating the beam in order to facilitate detection. A through-flow ionization detector possesses the versatility required for scattering studies using the time-of-flight technique. A sorption pump and a turbo pump serve as central components of alternative pumping systems for the collimating chamber.

All system components have been fabricated. Studies of energy and momentum exchange during collisions of molecules with solid surfaces will be initiated as soon as measurements of beam performance are completed.

Note Added in Proofreading: Using the arc-heated source, the converging nozzle, the conduction-radiation-cooled skimmer, the turbo pump (turning at 3400 rpm), the chopper-selector (acting only as a chopper), and the detector (all described in this report), an arc-heated beam was generated and detected on July 24, 1963.

## NOMENCLATURE

| | |
|---|---|
| $A$ | area |
| $b$ | larger dimension of rectangular orifice |
| $\bar{C}$ | mean of random molecular speeds |
| $d$ | characteristic dimension of skimmer orifice (either diameter of circular orifice or smaller dimension of rectangular orifice). |
| $F(u)$ | fraction of molecules per unit volume of velocity space |
| $G$ | intensity of molecular incidence on a surface |
| $h$ | enthalpy per unit mass |
| $I$ | molecular flux |
| $I(s)ds$ | molecular flux in speed range ds |
| $I(T_\Lambda)dT_\Lambda$ | molecular flux in transit-time range $dT_\Lambda$ |
| $k$ | Boltzmann's constant |
| $K$ | detector calibration constant [Equation (38)] |
| $Kn$ | Knudsen number ( $\equiv \lambda/d$) |
| $L$ | length |
| $m$ | mass of molecule |
| $M$ | Mach number [$\equiv U/(\gamma kT/m)^{1/2}$ for a perfect gas] |
| $n$ | number density of molecules |
| $N$ | number of molecules |
| $\dot{N}$ | flow rate of molecules |
| $p$ | pressure |
| $p_{eq}$ | equilibrium pressure in sorption pump for given sorbent temperature and for given quantity of sorbate sorbed |
| $R$ | resolution of chopper-selector $\equiv (s_{max} - s_{min})/s_\tau$ |
| $s$ | speed ratio $\equiv u/(2kT/m)^{1/2}$ |
| $\tilde{s}$ | most probable speed ratio |
| $s_{max}$ | maximum speed ratio of molecules transmitted by chopper-selector |
| $s_{min}$ | minimum speed ratio of molecules transmitted by chopper-selector |
| $s_\tau$ | speed ratio of those molecules with transit time equal to delay time of the chopper-selector rotor relative to the entrance section $\equiv \Lambda/\tau(2kT/m)^{1/2}$ |

| | |
|---|---|
| $S$ | speed ratio $\equiv U/(2kT/m)^{1/2}$ |
| $t$ | time |
| $T$ | temperature (absolute) |
| $T_{td}$ | time of flight from target to detector |
| $T_\Lambda$ | transit time for molecule passing through chopper-selector with length $\Lambda$ |
| $\mathcal{T}$ | fraction of admitted molecules transmitted by chopper-selector |
| $u$ | molecular speed |
| $U$ | speed corresponding to average velocity |
| $V$ | electrical potential |
| $W$ | through-flow ratio for turbo pump |
| $\alpha$ | sticking coefficient |
| $\beta$ | open time of chopper-selector slit $\equiv \theta/\omega$ |
| $\gamma$ | specific-heat ratio |
| $\Gamma$ | transmission function [Equation (24)] |
| $\delta_i$ | internal half-apex angle of skimmer |
| $\theta$ | chopper-selector slit-opening angle |
| $\lambda$ | mean-free-path length |
| $\Lambda$ | distance between entrance and exit sections of chopper-selector rotor |
| $\sigma$ | molecular collision cross-section |
| $\tau$ | delay time of the chopper-selector rotor relative to the entrance section $\equiv \phi/\omega$ |
| $\phi$ | relative angular displacement of entrance and exit sections of chopper-selector rotor |
| $\omega$ | angular speed |
| $\Omega$ | solid angle |

Subscripts

| | |
|---|---|
| o | stagnation conditions |
| 1 | first collimating orifice |
| 2 | second collimating orifice |
| b | beam |
| c | collimating chamber |
| d | detector |
| s | chopper-selector |
| t | target |

TABLE OF CONTENTS

## LIST OF FIGURES

## LIST OF FIGURES (Cont.)

Page

53

54

56

57

59

## LIST OF TABLES

## INTRODUCTION

The value of the molecular beam as a laboratory tool has been established firmly. For example, it has played key roles in experimental studies of velocity distributions in gases, structures of molecules, and collisions (both elastic and inelastic) of molecules with other molecules or with surfaces. (Cf. References 1-6.) However, all of the early beam sources consisted of enclosures (ovens) containing molecules at a temperature equal to the temperature of the enclosure walls and at a pressure such that the mean-free-path length of the molecules within the enclosure was greater than the characteristic dimension of the opening through which the molecules escaped. The most probable speed (proportional to the square root of the source temperature) of the escaping molecules was limited consequently by the maximum allowable temperature (approximately $3000^{\circ}K$) of the enclosure walls. For example, the most probable speed of nitrogen molecules escaping from an enclosure at $3000^{\circ}K$ is approximately 1600 m/sec - an order of magnitude less than either the speed of meteors, satellites and space vehicles or the minimum speed of approach of molecules required for many interesting chemical reactions. If the opening is a slit having width proportional to the mean-free-path length of the molecules within the enclosure, then the beam intensity is independent of the molecular density within the enclosure (i.e., independent of the slit width). Intensities of well-designed oven beams are of the order of $10^{14}$ molecules/$cm^2$-sec at a distance of 1 meter from the source. Higher intensities would facilitate detection of the beam after filtering out molecules with undesirable velocities and after scattering from targets.

As a consequence of the aforementioned speed and intensity limitations of conventional oven beams, several development programs have been initiated in recent years for the purpose of increasing the speed and/or the intensity of the molecular beam. A brief summary of the principal design features of those high-intensity beams (all using nozzle sources) known to the author is presented as Table I. The difficulty of generating and measuring a high-intensity high-speed beam is illustrated by the fact that, of the seven organizations with high intensity

TABLE I

PRINCIPAL DESIGN FEATURES OF SEVERAL HIGH-INTENSITY NOZZLE BEAMS

| Organization | Speed | Speed Filter | Detector | Initial Application | Comments | References |
|---|---|---|---|---|---|---|
| Cornell Univ. + Harvard | Average | None | Steady State Pirani | | Pioneering Effort; Discontinued | 7, 8 |
| Germany | High (Binary Beam) | None | Through-Flow Ionization | Thermal Relaxation | Single-Disk Chopper; Operational | 9-14 |
| Virginia | High[1] (Binary Beam) | Six-Disk | Steady-State Ionization | Surface Scattering | Rotating Target;[1] Development Continuing | 15-18 |
| Cornell Aero. Lab. | High (Shock Tube) | None | Mass Spectrometer[1] | Molecular Scattering | Double-Expansion Source; Development Continuing | 19 |
| Princeton | High[1] (Binary Beam) | Time-of-Flight[1] | Steady-State Ionization | Surface Scattering | Two-Stage Pumping; Development Continuing | 20-22 |
| France | High[1] (Ion Acceleration) | None | Steady-State Ionization | Surface Scattering | Also Hot-Tungsten Detector; Development Continuing | 23 |
| Grumman Aircraft | High[1] (Shock Tube) | None | Through-Flow Ionization | Surface Scattering | Array of Detectors;[1] Development Continuing | 24, 25 |
| UCLA | High[1] (Arc-Heated) | Two-Disk | Through-Flow Ionization | Surface Scattering | Combined Filter-Chopper; Development Continuing | |

1. This component or feature does not appear to have been operational at the time the latest available report

and high speed as major objectives, only two (Germany and Cornell Aero. Lab.) are known to have generated and measured relatively high intensities and speeds even though the median elapsed development time for these seven programs is of the order of five years.

Four additional organizations are known to have plans for developing high-intensity nozzle beams. The University of Toronto Institute of Aerophysics[26] plans to use a binary (hydrogen-nitrogen) beam, a thermal-expansion strip target and a torsional microbalance in studies of surface interactions; the molecular-beam group at the University of California at Berkeley Institute of Engineering Research[27] plans to set up a nozzle beam (with two-disk speed filter) in the low-density wind tunnel; the Applied Physics Laboratory at Johns Hopkins University plans to study chemical reactions using a beam generated by a porous-walled nozzle and modulated at 100 cycles per second with a 1% duty cycle;[28] and the General Electric Company plans to use a beam heated by an electric arc and pumped by a cryogenic surface in studies of momentum and energy transfers in collisions of atoms with solid surfaces.[29] Design features of these beams are omitted from Table I pending construction of system components.

An alternative suggestion for increasing beam intensity is to use multiple sources. Zacharias and Haun[30] suggest using multiple channels formed by a stack of either hypodermic needles or channel-crimped foil; Datz, Minturn and Taylor[31] suggest using multiple orifices formed by electro-formed nickel mesh. A procedure for combining this method for producing high intensity with known methods for producing high speeds is not apparent however.

Several investigators (e.g., Fite et al, References 32 and 33) reduce the need for higher intensity by using a modulated beam in order to facilitate separating beam effects from background effects. Although they use this technique in connection with oven beams, no limitations prohibiting its use in high-speed beams are obvious.

1. This component or feature does not appear to have been operational at the time the latest available report describing this beam was written.

In the following sections of this report, the current status of the molecular beam being developed at UCLA is reviewed briefly. Although the arc-heated source has not been tried yet in the beam, a description of those system components which are operational and a record of those development experiences which might be of interest to contemporary investigators is believed to be appropriate at this time.*

## PRINCIPAL DESIGN FEATURES, UCLA NOZZLE BEAM

A brief composite description of the principal design features of the high-speed high-intensity molecular beam being developed at UCLA is provided here as an introduction to the individual descriptions of the several system components and development experiences which follow. Perhaps this composite description will coordinate and give added meaning to the individua descriptions.

First, however, comments concerning the environment in which this facility is being developed, and a development philosophy which has evolved as a consequence of this environment, appear to be in order. All of the development work is being done either by a full-time member of the academic staff or by graduate students with the assistance of undergraduate students; no professional research employees are involved. In this respect, the situation is similar perhaps to the situation at other engineering or science schools. However, most of the graduate students in the Department of Engineering at UCLA are part-time students and also part-time employees in the local engineering industries (largely aerospace and electronics industries). Hence although the engineering graduate student at UCLA is frequently relatively mature and highly motivated, he is, at the same time, frequently progressing less rapidly towards his degree than is the average graduate student in the United States. As a consequence, in the subject development program, simultaneous studies of alternative methods are undertaken frequently - particularly if one (or both) of the methods is novel, if the added expense of the second study is not prohibitive, and if the addition of the second study does no slow up significantly the progress on the first study. Evidence of this

*See Note Added in Proofreading, p. iii.

development philosophy appears in the descriptions which follow.

The vacuum system resembles the majority of molecular-beam vacuum systems in that it is divided into three chambers - a source chamber, a collimating chamber and a detecting chamber - each with its own pumping system. (Cf. Figure 1.) If the maximum allowable pressures for the three chambers differ significantly from each other, then use of three different pumping systems minimizes the required combined pumping capacity. Some molecular-beam vacuum systems (e.g., References 20-22) are divided into only two chambers - a source chamber and a combined collimating and detecting chamber - using only two pumping systems. Such an arrangement requires that the entire gas load from the combined collimating and detecting chamber be pumped at the maximum pressure allowable in the vicinity of the detector, i.e., it requires a larger combined pumping capacity.

The beam source is an arc-heated hypersonic jet. High molecular speeds (in excess of 1 ev) are expected as a consequence of heating the beam gas in the electric arc and converting then the energy of thermal motion into energy of directed motion in the hypersonic jet. High beam intensities (of the order of $10^{16}$ molecules/$cm^2$-sec) are expected as a consequence of converting the thermal motion into directed motion in the hypersonic jet. Two alternative methods are being studied. In the first method, the hypersonic jet is formed by expansion through a converging-diverging nozzle and the pumping capacity required for the source chamber is reduced by partial recovery of stagnation pressure in a hypersonic diffuser. In the second method, the hypersonic jet is formed by expansion through a converging nozzle and a free jet; if recovery of stagnation pressure as a result of flows through shocks is negligible, then the gas load from the source chamber must be pumped at the static pressure in the free jet, i.e., a larger pumping capacity is required than in the first method. Available information on low-density flows in channels and in free jets indicates that the second method has the greater probability of success. Furthermore, means for adjusting the source location are incorporated more easily into the second method.

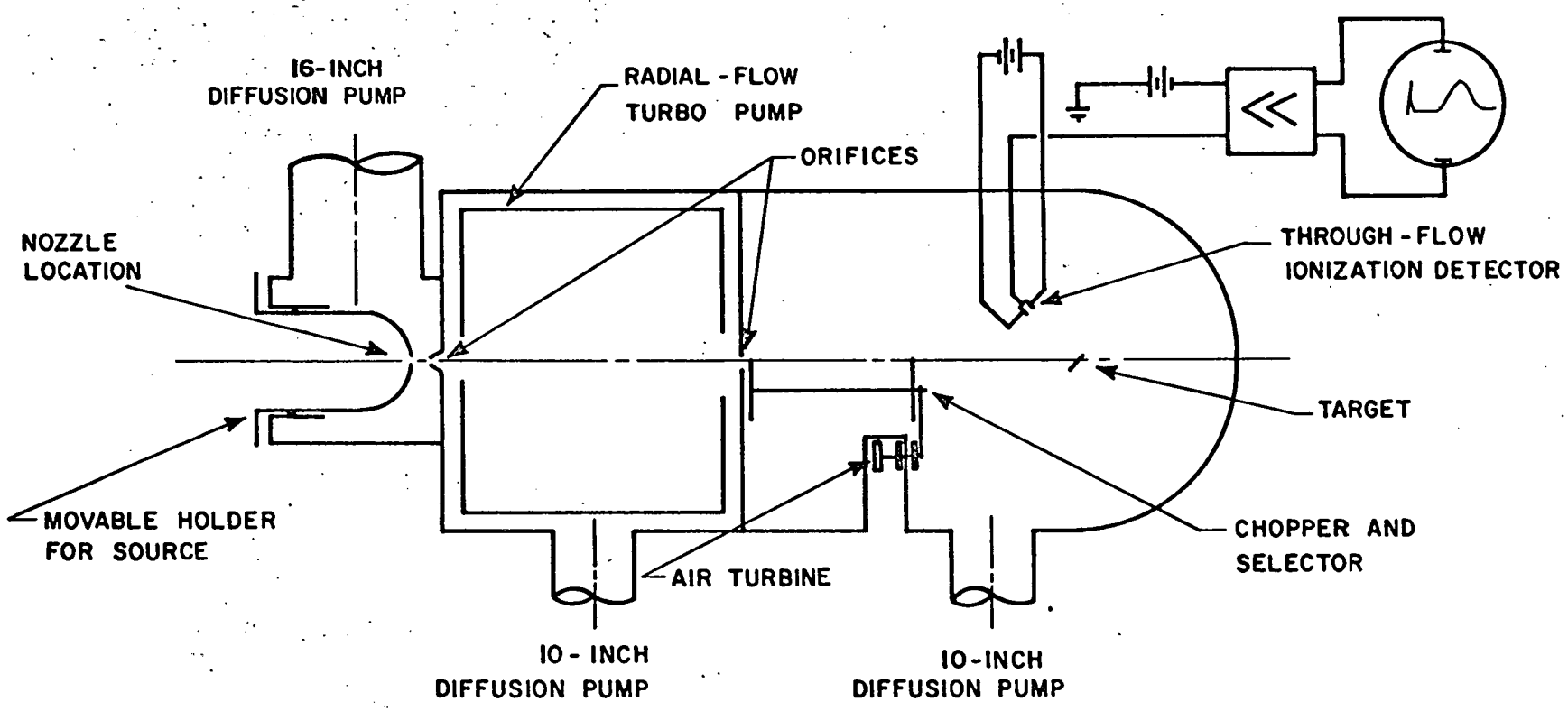


SCHEMATIC DIAGRAM OF UCLA NOZZLE BEAM

FIGURE 1

FIGURE 1 SCHEMATIC DIAGRAM OF UCLA NOZZLE BEAM

Beam collimation is provided by two circular orifices, the first orifice located in a conical skimmer placed in the hypersonic jet and the second orifice located in the wall separating the collimating and detecting chambers. Two alternative designs of the conical skimmer are considered. The first design incorporates passages for cooling water with the result that the external cone angle is relatively large. The second design depends upon conduction and radiation for removal of heat with the result that the external cone angle can be made smaller. Since attenuation of beam intensity is reduced when the external cone angle is reduced, the smallest external cone angle consistent with requirements for fabricating and cooling the skimmer is to be used.

A two-disk beam chopper and speed selector provides a means for analyzing the speed distribution in the generated beam, for chopping the beam into bursts of nearly monoenergetic molecules suitable for scattering studies using the time-of-flight technique and for modulating the beam in order to facilitate detection. A wide continuous range of angular rotor speeds is available through use of an air-turbine drive. The need for a rotating seal is obviated by transmitting torque from the turbine to the chopper-selector rotor by permanent magnets rotating on both sides of a non-ferrous insert in the vacuum-chamber wall. Location of the chopper-selector in the collimating chamber is prohibited by the presence of either the sorption pump or the turbo pump in that chamber.

As indicated in the preceding paragraph, scattering studies using the time-of-flight technique are planned. This technique requires measurements from which the time-of-flight of molecules between two points (e.g., between a target and a detector or between two detectors) may be computed. The through-flow ionization detector of Becker et al[12] appears to be suited best for this purpose. Hence, a slightly modified version of this detector has been developed for use in these studies. Use of a mass spectrometer[19, 32, 33] is kept in mind as a supplementary detection method.

Conventional oil-diffusion and mechanical pumps are used for the source and detecting chambers. However, if baffled oil-diffusion pumps were used for the collimating chamber, then at least one (perhaps two) 32-inch diffusion pump

would be required. It was eliminated from consideration by its high initial cost relative to total grant funds and by its bulk. Cryogenic pumps were eliminated either due to high operating costs (in the case of liquid helium or liquid neon) or due to high explosion hazards (in the case of liquid hydrogen). Preliminary calculations revealed, however, that either a sorption pump cooled with relatively inexpensive liquid nitrogen or a two-stage radial-flow turbo pump might have the required pumping speed as well as modest initial and operating costs. Relative to each other, the sorption pump has the disadvantage of requiring periodic desorption whereas the turbo pump has the disadvantage of a higher initial cost (nearly half the cost of a 32-inch diffusion pump installed). Since both pumping systems are novel, since University funds were available for the turbo-pump development, and since the two development programs could be conducted independently by two different graduate students, both development programs were undertaken. These programs have shown that both pumping systems are feasible. Hence, as a consequence of the disadvantage of the periodic desorption required by the sorption pump, it is expected that the turbo pump will be used more frequently than the sorption pump in the subject molecular beam.

The vacuum system, arc-heated source, converging-diverging nozzle, converging nozzle, hypersonic diffuser, water-cooled skimmer, conduction-radiation-cooled skimmer, flat-plate collimating orifice, two-disk beam chopper and speed selector, detector, sorption pump and turbo pump have been fabricated. The arc-heated source and converging-diverging nozzle have been tested exhausting at room pressure whereas the source and converging nozzle have been tested exhausting at source-chamber pressures of the order of $10^{-2}$ torr; the chopper-selector has been operated routinely at speeds up to 4600 rpm in detector calibrations; the detector has been calibrated using chopped room-temperature effusive flows; the sorption pump is operational;[34] and the turbo pump has performed satisfactorily at rotational speeds up to 67% of designed rotational speed (higher speeds have not been tested).* More detailed description of system components and development experiences are included in the following sections of this report and in the several theses[35-42] which have been completed in the Molecular-Beam Laboratory.

*See Note Added in Proofreading, p. iii.

## BEAM-SOURCE

The design of the arc-heated beam source is the result of an effort to provide high beam energies and high beam intensities subject to constraints imposed by material properties, fabrication techniques, and equipment characteristics. If the jet expands to Mach numbers large in comparison with unity, then the kinetic energy of a beam molecule is given to good approximation by

$$\frac{1}{2} m U^2 \approx m h_o \tag{1}$$

where m is mass of molecule, U is speed corresponding to average velocity, h is enthalpy per unit mass, and subscript o refers to stagnation conditions. For a perfect monatomic gas, Equation (1) becomes

$$\frac{1}{2} m U^2 \approx \frac{5}{2} k T_o \tag{1a}$$

where k is Boltzmann's constant and T is temperature. The discussion of the beam intensity at the second collimating orifice is facilitated by examining

$$I_2 = I_1 A_1 \frac{I_2 A_2}{I_1 A_1} \frac{1}{A_2} \tag{2}$$

where I is molecular flux (molecules per unit area and per unit time), A is area, and subscripts 1 and 2 refer respectively to the first and second collimating orifices. In practice, the flow rate $I_1 A_1$ through the first orifice is limited by the pumping capacity for the collimating chamber. For a perfect gas, this flow is related to stagnation conditions and to Mach number at skimmer entrance (see any text book describing quasi-one-dimensional compressible flows) by

$$I_1 A_1 = \frac{p_o}{k T_o} \left(\gamma \frac{k T_o}{m}\right)^{1/2} A_1 \frac{M_1}{\left(1 + \frac{\gamma - 1}{2} M_1^2\right)^{(\gamma+1)/2(\gamma-1)}} \tag{3}$$

where p is pressure, $\gamma$ is specific-heat ratio and M is Mach number [$\equiv U/(\gamma k T/m)^{1/2}$ for perfect gas]. Since free-molecule flow conditions are

required at the skimmer entrance, the characteristic dimension of the skimmer orifice may be written conveniently as a function of stagnation conditions, Mach number, Knudsen number and molecular properties using

$$Kn_1 = \frac{\lambda_1}{d_1} = \frac{1}{\sqrt{2}\, n_1 \sigma d_1} = \frac{1}{\sqrt{2}\, n_o \sigma d_1} \left(1+\frac{\gamma-1}{2} M_1^2\right)^{1/(\gamma-1)} \tag{4}$$

where $Kn \equiv \lambda/d$ is Knudsen number, $\lambda$ is mean-free-path length, d is characteristic dimension of skimmer orifice, n is number density of molecule and $\sigma$ is molecular collision cross-section. Combining Equations (3) and (4), one obtains for a circular orifice with diameter d

$$I_1 A_1 = \left(\gamma \frac{kT_o}{m}\right)^{1/2} \frac{\pi kT_o}{8 p_o \sigma^2} \frac{\left(1+\frac{\gamma-1}{2} M_1^2\right)^{(3-\gamma)/2(\gamma-1)} M_1}{Kn_1^2} \tag{5}$$

and for a rectangular orifice with smaller dimension d and large dimension b

$$I_1 A_1 = \left(\gamma \frac{kT_o}{m}\right)^{1/2} \frac{b}{\sqrt{2}\,\sigma} \frac{M_1}{\left(1+\frac{\gamma-1}{2} M_1^2\right)^{1/2} Kn_1} \tag{6}$$

For a monatomic gas ($\gamma = 5/3$) and $M_1 >> 1$, these two equations may be written respectively

$$I_1 A_1 \approx \left(\frac{5}{3}\right)^{1/2} \frac{\pi}{24} \left(\frac{kT_o}{m}\right)^{1/2} \frac{kT_o}{p_o \sigma^2} \frac{M_1^3}{Kn_1^2} \tag{5a}$$

and

$$I_1 A_1 \approx \left(\frac{5}{2}\right)^{1/2} \left(\frac{kT_o}{m}\right)^{1/2} \frac{b}{\sigma} \frac{1}{Kn_1} \tag{6a}$$

The remaining factor in Equation (2) may be written (Reference 15, Equations 7 and 8)

$$\frac{I_2 A_2}{I_1 A_1} \frac{1}{A_2} = \frac{\sqrt{\pi}\; S(1+\mathrm{erf}\, S)\left(S^2+\frac{3}{2}\right) + e^{-S^2}(1+S^2)}{\sqrt{\pi}\; S(1+\mathrm{erf}\, S) + e^{-S^2}} \frac{1}{\pi L_{12}^2} \tag{7}$$

where $S \equiv U/(2kT/m)^{1/2}$ is speed ratio and $L_{12}$ is distance between the two orifices. For $S >> 1$,

$$\frac{I_2 A_2}{I_1 A_1} \frac{1}{A_2} \approx \frac{S^2}{\pi L_{12}^2} \tag{7a}$$

Equation (1a) indicates that high beam energies are realized for high stagnation temperatures; Equations (2) and (7a) indicate that high beam intensities are realized for high flow rates through the skimmer orifice for high speed ratios (i.e., high Mach numbers) and for small distances between orifices. Equations (5) and (6) relate the flow rate through the skimmer orifice to stagnation conditions, Knudsen number, Mach number (circular orifice only) and dimension b (rectangular orifice only).

Argon has been selected as the working fluid for the initial experiments. It is relatively simple (a monatomic gas), has been investigated extensively, is easy to handle, and is available readily. Initial design of the facility is based upon a stagnation enthalpy of 700 cal/gm (5700°K), a flow rate of $10^{19}$ atoms per second through the skimmer orifice, a Mach number at skimmer entrance of 10, and a distance of 1 meter between orifices. These conditions place relatively modest requirements upon material properties, pumping capacities and collimating-chamber pump geometry.

Examine now the design implications of Equations (5) and (6). For the design conditions of the preceding paragraph, these equations may be written

$$Kn_1 = 9.2\, p_o^{-1/2} \tag{5b}$$

and

$$Kn_1 = 4.7\, b_1 \tag{6b}$$

where $p_o$ is in torr and $b_1$ is in cm. In order to avoid the formation of a shock at the skimmer entrance, the Knudsen number must be at least as large as unity - and perhaps as large as 10.[22] From Equations (4), (5b) and (6b), one obtains, for Knudsen numbers of 1 and 10, the requirements on stagnation

pressure and skimmer orifice indicated in Table II. Since the stagnation pressure (85 torr) and orifice diameter (0.27 cm) computed for the circular orifice for Knudsen number of unity are obtained easily, and since a circular orifice is fabricated more easily than a rectangular orifice, a circular orifice is to be used in tests with Knudsen numbers of the order of unity. However, since the stability of the electric arc at pressures less than 10 torr is unknown the rectangular orifice might be preferred if operation at Knudsen numbers of the order of 10 is required. Initial tests will be made at a stagnation pressure of 100 torr and using a circular skimmer orifice with a diameter of 0.25 cm, i.e., at a Knudsen number of the order of unity.

The diameter of the throat through which the arc-heated jet expands is a compromise between the capacity of the pumping system for the source chamber and the operating characteristics of the arc-heated source. If the diameter is too large, then the design of a source-chamber pumping system with sufficient capacity becomes impractical; if the diameter is too small, then one is likely to encounter either arc instabilities or excessive energy losses from the jet to the nozzle surfaces. A throat diameter of 0.2 cm is to be used in the initial tests. This diameter, combined with a stagnation temperature of $5700^{\circ}K$ and a stagnation pressure of 100 torr, leads to a mass-flow rate of 101 grams per hour. Heating this gas stream requires a power input of 0.079 KW to the gas stream, a modest power requirement.

Fundamental in the design of the beam are the conditions at the skimmer entrance. For the design conditions specified in the preceding paragraphs ($T_o = 5700^{\circ}K$, $p_o = 100$ torr, and $M_1 = 10$), one obtains, at the skimmer entrance, a temperature of $166^{\circ}K$, a pressure of 0.0145 torr and a speed of 2400 m/sec (1.2 ev/atom). Since the equilibrium degree of ionization for argon at $5700^{\circ}K$ and 100 torr is of the order of 0.0001, it is anticipated that the degree of ionization at the skimmer entrance will be less than 0.0001. (A quantitative prediction of the degree of ionization at the skimmer entrance is difficult to obtain due to non-equilibrium effects. Cf. Reference 38.) Any ions and electrons remaining in the stream at the skimmer entrance can be deflected out of the beam using either an electric or a magnetic field. According

TABLE II

REQUIREMENTS ON STAGNATION PRESSURE AND SKIMMER ORIFICE FOR TWO VALUES OF KNUDSEN NUMBER

| | Circular Orifice | | Rectangular Orifice | |
|---|---|---|---|---|
| $Kn_1$ | $p_o$ (torr) | $d_1$ (cm) | $b_1$ (cm) | $p_o d_1$ (torr-cm) |
| 1 | 85 | 0.27 | 0.21 | 23 |
| 10 | 0.85 | 2.7 | 2.1 | 2.3 |

Kn = Knudsen number $\equiv \lambda/d$

$\lambda$ = mean-free-path length

d = characteristic dimension (either diameter of circular orifice or smaller dimension of rectangular orifice)

b = larger dimension of rectangular orifice

p = pressure

Subscripts o and 1 refer respectively to stagnation and skimmer-entrance conditions.

Calculations are for argon, a stagnation temperature of 5700°K, a flow rate of $10^{19}$ atoms per second through the skimmer office and a Mach number at skimmer entrance of 10.

to information received from Giannini Plasmadyne Corporation of Santa Ana, California, if a noble gas and a water cooled tungsten back electrode is used, then the electrode decomposition rate is less than one gram in 1000 kilowatt-hours. For gas-flow rates typical of the present facility, this electrode-decomposition rate would result in a contamination of less than one part tungsten in 100,000 parts working fluid. Hence, the beam is expected to be essentially a neutral beam of argon atoms.

Two alternative methods of forming the hypersonic jet are being studied. In the first method (Figure 2) it is formed by expansion through a converging-diverging nozzle. In an effort to reduce the pumping capacity required for the source chamber, that portion (98%) of the hypersonic jet which does not enter the skimmer is channeled through a constant-area hypersonic diffuser[40] which turns the flow into the radial direction and dumps it into a toroidal collector evacuated by a single-stage mechanical vacuum pump. Since a constant-area supersonic diffuser yields approximately the same pressure recovery as a normal shock,[43, p. 130] the pressure at the diffuser exit would be of the order of 2 torr. Hence, the volume flow at this pressure would be two orders of magnitude smaller than the volume flow at the static pressure realized in the vicinity of the skimmer entrance.

In the second method of forming the hypersonic jet (Figure 3), the arc-heated gas is expanded through a converging nozzle to a Mach number of unity and then through a free jet to hypersonic speeds. Applicable studies of free jets include the analytical studies of Owen and Thornhill,[44] Love, Grigsby, Lee and Woodling,[45] Eastman and Radtke,[46] Sherman,[47] and the exp mental studies of Wilcox, Weir, Nicholls and Dunlap,[48] Love et al,[45] Bier and Schmidt,[14] and Reis.[49] The analytical computations of Love et al and Sherman and the experimental results of Bier and Schmidt have particular value in the present studies since they include quantitative values for monatomic gases ($\gamma = 1.67$). If recovery of stagnation pressure as a result of flows through shoc is negligible, then the gas load from the source chamber must be pumped at the static pressure in the free jet, a pressure of the order of $10^{-2}$ torr. The volume flow at this pressure is two orders of magnitude greater than for the

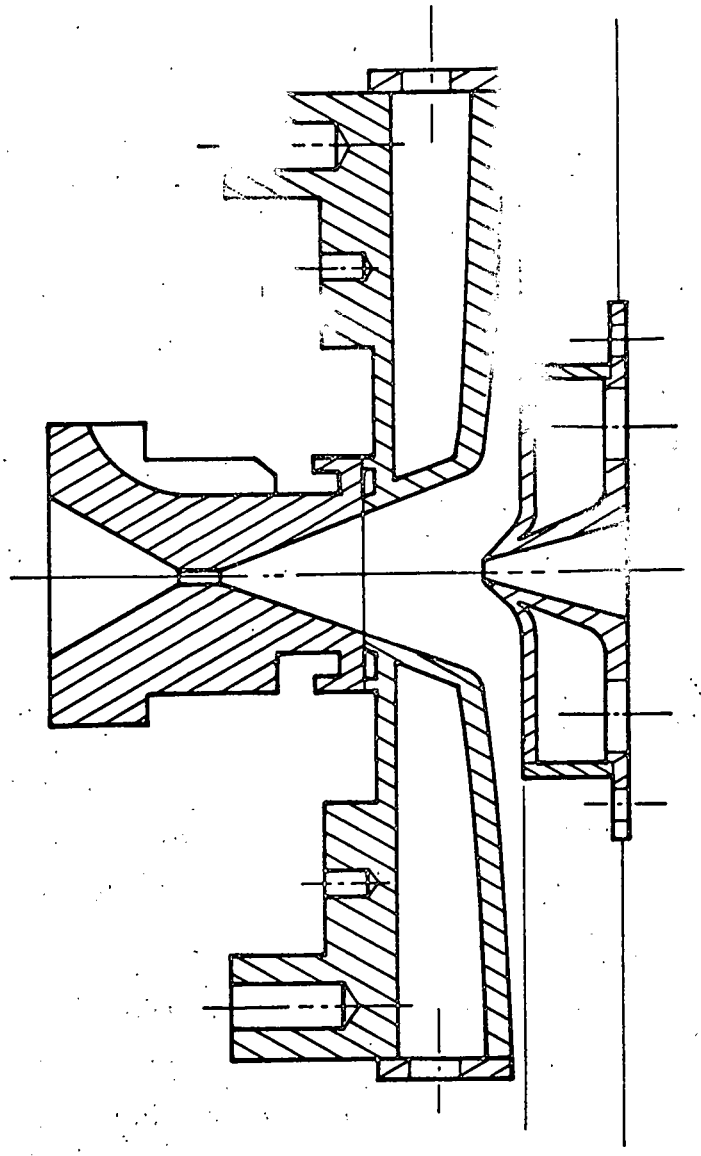

SCHEMATIC DIAGRAM OF HYPERSONIC NOZZLE,
CONSTANT-AREA DIFFUSER AND WATER-COOLED SKIMMER
(Ref. 35, Figure C-7)

FIGURE 2

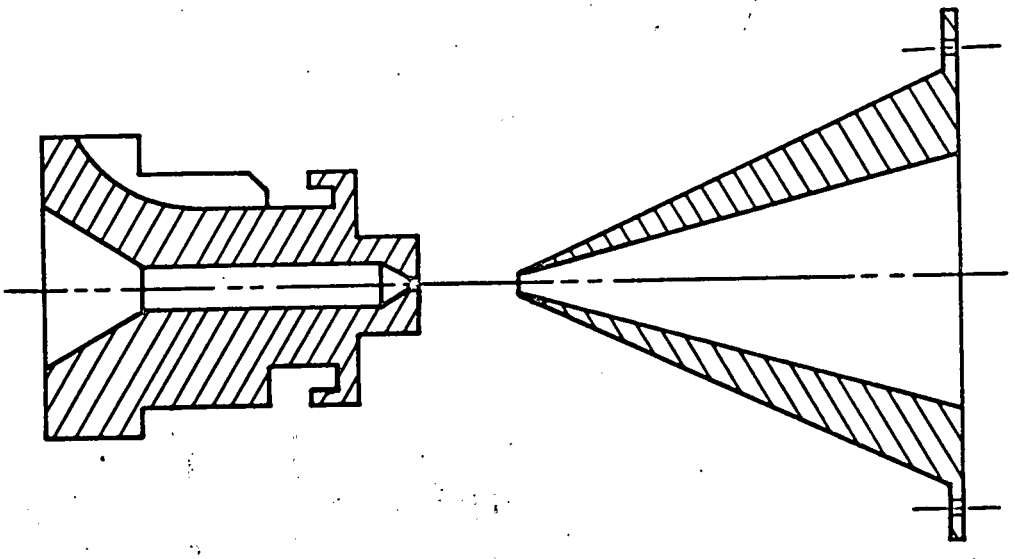

SCHEMATIC DIAGRAM OF SONIC NOZZLE,
FREE JET AND CONDUCTION-
RADIATION-COOLED SKIMMER

FIGURE 3

first method. However, recent successes with free jets at Princeton[20-22] and in Germany,[14] and the difficulties of handling rarefied hypersonic flows in channels,[40] indicate that the second method has the greater probability of success. Furthermore, the incorporation of means for adjusting the source location appears to be practical for the second method and impractical for the first method.

All of the source components (source chamber, arc-heated source, converging-diverging nozzle, hypersonic diffuser and converging nozzle) have been fabricated. The arc-heated source, a modification of the P-110B Plasmatron System (including a PS-20 power unit and an M4 head) manufactured by the Giannini Plasmadyne Corporation of Santa Ana, California, would be used regardless of which of the two alternative methods of forming the jet is selected. (See Figure 4 for a schematic diagram of the source electrodes.) This Plasmatron System, with the converging-diverging nozzle installed, has been tested exhausting at room pressure with argon-flow rates from approximately 300 to 1600 gm/hr at a power input of 2KW to the head. With the converging nozzle installed, it has been tested exhausting at source-chamber pressures of the order of $10^{-2}$ torr with argon-flow rates from 200 to 300 gm/hr at a power input of 2KW to the head and with argon-flow rates from 100 to 200 gm/hr at a power input of 4KW to the head; stagnation pressures varied from 80 to 180 torr. (Since a large fraction of the power input to the head was carried away by cooling water, only a small fraction of this power was added to the argon stream.) Stable operation was realized over the range of operating conditions tested.*

## BEAM COLLIMATOR

As indicated in preceding sections of this paper, beam collimation is provided by two circular orifices, the first orifice located in a conical skimmer placed in the hypersonic jet and the second orifice located in the wall separating the collimating and detecting chambers. In this section, collimator design details and beam attenuations due to scattering are discussed.

*See Note Added in Proofreading, p. iii.

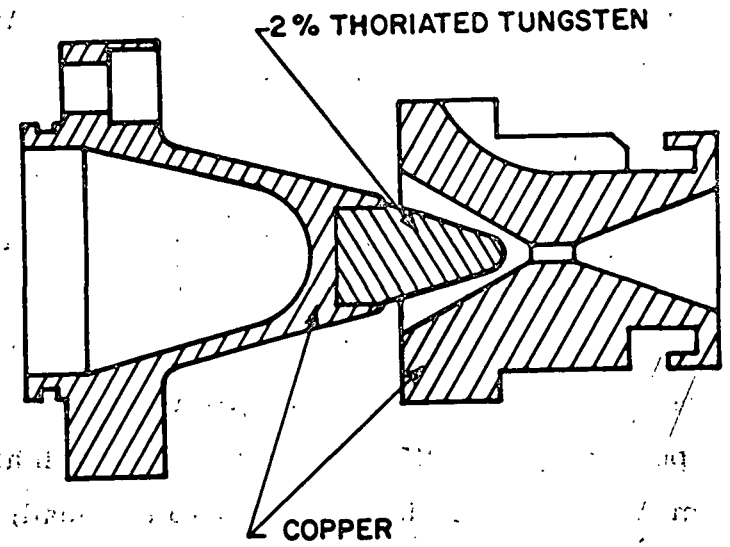


SCHEMATIC DIAGRAM OF SOURCE ELECTRODES
(Ref. 35, Figure C-4)

FIGURE 4

The distance between the two orifices (i.e., the length of the collimating chamber) is approximately 1 meter. This value represents a compromise between the requirement for high beam intensity (cf. Equation 7a) and the requirement imposed by collimating-chamber pump geometry (cf. section on vacuum pumps).

As indicated in the discussion of the design of the beam source, initial tests will be made using a circular skimmer orifice with a diameter of 0.25 cm. Using argon at a stagnation enthalpy of 700 cal/gm (5700°K), a stagnation pressure of 100 torr and a Mach number at skimmer entrance of 10, this value of diameter provides a flow rate of $10^{19}$ atoms per second through the skimmer orifice and a Knudsen number of the order of unity. If (as suggested in Reference 22) a Knudsen number of the order of 10 is required, then (in order to maintain the flow rate of $10^{19}$ atoms per second and a relatively high stagnation pressure) one might use a rectangular orifice with dimensions of the order of 2 cm x 0.2 cm and reduce the stagnation pressure to 10 torr (cf. Table II).

Requirements for reducing the attenuation of beam intensity due to scattering by atoms reflected from skimmer surfaces place conflicting demands upon the angles of the inner and outer surfaces of a conical skimmer; increasing the internal angle reduces attenuation due to scattering by atoms reflected from the internal surface whereas decreasing the external angle reduces attenuation due to scattering by atoms reflected from the external surface. Kantrowitz and Grey[7] suggest, for the internal angle,

$$\delta_i \geq \sin^{-1} (\bar{C}_1/U) \tag{8}$$

where $\delta_i$ is internal half-apex angle and $\bar{C}$ is mean of random molecular speeds. As guides in the selection of the external angle, one might use values of the maximum cone and wedge angles for shock attachment and the calculations of Oman[24] which predict that, for attenuations less than 30%, the attenuation due to atoms reflected from the external surface varies exponentially with the external angle. Figure 5 indicates that, for argon and a Mach number of 10,

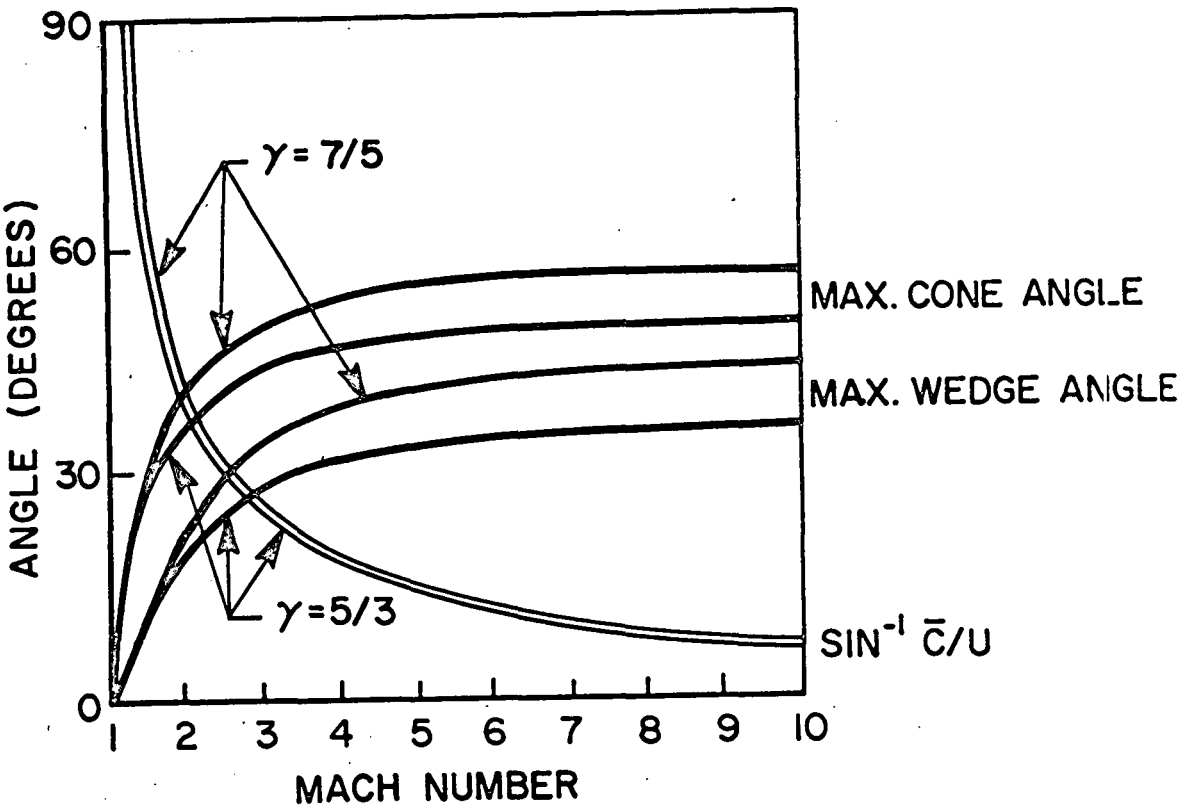


CRITICAL ANGLES FOR DESIGN OF SKIMMER

FIGURE 5

$\sin^{-1}(\bar{C}_1/U) = \sin^{-1}(\sqrt{\delta/\pi\gamma}/M_1) = 7^\circ$ whereas maximum half-apex angles for shock attachment are $50^\circ$ for a cone and $36^\circ$ for a wedge. Since the steady-state temperature of the lip of a skimmer placed in an arc-heated jet is difficult to predict, two alternative designs of the skimmer are considered. The first design incorporates passages for cooling water; internal and external half-apex angles are respectively $15^\circ$ and $45^\circ$, i.e., the external angle is relatively large. (Cf. Figure 2.) The second design depends upon conduction (to the water-cooled skimmer base) and upon radiation for removal of heat; internal and external half-apex angles are respectively $15^\circ$ and $25^\circ$, i.e., the external angle can be made relatively small. (Cf. Figure 3.) Since attenuation of beam intensity is reduced when the external angle is reduced, the smallest external angle consistent with requirements for fabricating and cooling the skimmer is to be used.*

An upper bound to the cooling required for the skimmer is provided by the power added to the gas stream by the arc, i.e., 0.079 KW. Only a modest water-flow rate is required to carry away energy at this rate. The problem is to conduct heat away from the sharp skimmer lip without excessively high temperatures at the lip. Although preliminary calculations indicate that these temperatures will not be excessive, the final design will be based upon results of experimental tests.

The second (collimating) orifice is a circular hole, with diameter of 0.64 cm, located in a thin plate mounted in the wall separating the collimating and detecting chambers. Increasing the diameter of this orifice would increase the flow rate of molecules striking the target and, hence, would increase the flux of scattered molecules at distances from the target large in comparison with the diameter of the target impact area. (See Table III for a summary of predicted values of beam intensities, flow rates and densities at key points in the beam.) The resulting gain in strength of the detector signal would be realized, however, at the expense of loss in resolution; the larger the diameter of the target impact area, the greater is the uncertainty of the path length traversed by a molecule between the time it strikes the target and the time it passes through the detector.

---

*See Note Added in Proofreading, p. iii.

TABLE III

PREDICTED VALUES OF BEAM INTENSITIES, FLOW RATES AND DENSITIES AT KEY POINTS IN UCLA NOZZLE BEAM

| | Intensity $\left(\frac{\text{molecules}}{\text{cm}^2\text{-sec}}\right)$ | Flow Rate $\left(\frac{\text{molecules}}{\text{sec}}\right)$ | Density $\left(\frac{\text{molecules}}{\text{cm}^3}\right)$ |
|---|---|---|---|
| Skimmer | $2.0 \times 10^{20}$ | $1.0 \times 10^{19}$ | $8.4 \times 10^{14}$ |
| Collimator | $2.7 \times 10^{16}$ | $8.6 \times 10^{15}$ | $1.1 \times 10^{11}$ |
| Target | $6.8 \times 10^{15}$ | $8.6 \times 10^{15}$ | $2.7 \times 10^{10}$ |
| Detector | $6.9 \times 10^{12}$ | $8.7 \times 10^{12}$ | $1.5 \times 10^{8}$ |

Calculations are for argon, stagnation temperature of 5700°K, stagnation pressure of 100 torr, Mach number at skimmer entrance of 10, skimmer-orific diameter of 0.25 cm, collimating-orifice diameter of 0.64 cm, detector opening diameter of 1.27 cm, distance between orifices of 100 cm, distance from secon orifice to target of 100 cm, distance from target to detector of 20 cm, target temperature of 300°K, complete accommodation at target, detector on (or near) line normal to target, no speed filter, and negligible background or self scattering.

Since a relatively high beam intensity at the target is essential in many beam experiments, an estimate of beam attenuation due to background and self scattering is of interest. Consider first background scattering, i.e., scattering due to collisions of beam molecules with those molecules moving randomly about within the collimating chamber. To good approximation, each collision of a beam molecule with a background molecule leads to removal of one molecule from the beam; additions of molecules to the beam as a consequence of collisions involving background molecules are negligible. The probability that a beam molecule will undergo a collision as it traverses a path length dL is given by $dL/\lambda_c$, where $\lambda_c$ is mean-free-path length for beam molecules considering only collisions with the background molecules. For a high-speed molecule moving through a swarm of low-speed molecules, $\lambda_c = 1/n_c\sigma$ where $n_c$ is number density of particles in the collimating chamber. Consider now self scattering, i.e., scattering due to collisions of beam molecules with beam molecules. To good approximation, each collision of a beam molecule with a beam molecule leads to removal of two molecules from the beam. The probability that a beam molecule will undergo a collision as it traverses a path length dL is given by $dL/\lambda_b$, where $\lambda_b$ is mean-free-path length for beam molecules considering only collisions with beam molecules. Muckenfuss[50] has shown that if $M_1 >> 1$ and if the three-dimensional nature of the random thermal motions within the beam must be considered, then $\lambda_b = (1/\sqrt{2}\ n_b\sigma)(U/\bar{C}_b)$ where $n_b$ is the number density of the beam molecules and $\bar{C}_b$ is the mean random thermal speed of the beam molecules. Troitskii[51] has shown that if the beam is so narrow, in comparison with the mean-free-path length $\lambda_b$, that only the random thermal motions in the axial direction need be considered, then the mean-free-path length $\lambda_b$ is three times greater.[51] Preliminary calculations indicate that, for the present design, the beam width is small in comparison with the mean-free-path length $\lambda_b$, even in the collimating chamber. Hence, adding the two probabilities,

$$\frac{dN}{N} = -\frac{dL}{\lambda_c} - 2\frac{dL}{\lambda_b}$$

$$= -n_c\sigma\, dL - (2\sqrt{2}/3)\, n_b\sigma\,(\bar{C}_b/U)dL \qquad (9)$$

Neglecting losses due to scattering, the number density of beam molecules varies inversely as the square of the distance L from an equivalent point source with strength and location (upstream of first orifice) such that the number densities of beam molecules at the first and second orifices are respectively $n_1$ and $n_1 A_1 S^2/\pi L_{12}^2$ when $S>>1$. To the extent that $(A_1/\pi)^{1/2} S$ is negligible in comparison with $L_{12}$, one may write

$$n_b = n_1 \frac{A_1 S^2}{\pi L^2} \tag{10}$$

and locate the first orifice at $L = (A_1/\pi)^{1/2} S$ and the second orifice at $L = L_{12}$. If losses due to scattering are taken into account, then

$$n_b = n_1 \frac{A_1 S^2}{\pi L^2} \frac{N}{N_1} \tag{11}$$

where $N/N_1$ is the fraction of those beam molecules passing through the skimmer and surviving at path length L. Substituting from Equation (11) into Equation (9), one obtains

$$\frac{dN}{N} = - n_c \sigma \, dL - \frac{2\sqrt{2}}{3} n_1 \frac{A_1 S^2}{\pi L^2} \frac{N}{N_1} \sigma \frac{\bar{C}_b}{U} dL \tag{12}$$

The variables N and L do not appear to be separable in general. Useful information is obtained, however, by examining two special cases. If self scattering is negligible, then

$$\frac{N_2}{N_1} = e^{-n_c \sigma L_{12}} \tag{13}$$

whereas, if background scattering is negligible, then

$$\frac{N_1 - N_2}{N_2} = \frac{2\sqrt{2}}{3} n_1 \frac{A_1 S^2}{\pi} \sigma \frac{\bar{C}_b}{U} \left( \frac{1}{(A_1/\pi)^{1/2} S} - \frac{1}{L_2} \right)$$

Neglecting $(A_1/\pi)^{1/2} S$ in comparison with $L_2$, the latter equation may be written

$$\frac{N_1 - N_2}{N_2} = \frac{4}{3}\left(\frac{2}{\pi}\right)^{1/2} n_1 \sigma \left(\frac{A_1}{\pi}\right)^{1/2} \qquad (14)$$

For $n_1 = 8.4 \times 10^{14}$ molecules/cm$^3$, argon, and skimmer-orifice diameter of 0.25 cm, Equation (14) predicts an attenuation of 29% due to self scattering whereas, for $T_c = 300^{\circ}$K, argon, and $L_{12} = 100$ cm, Equation (13) indicates that an attenuation of 11% due to background scattering is realized if $p_c = 1.0 \times 10^{-5}$ torr. The 29% attenuation due to self scattering is accepted as a consequence of high intensity; the collimating-chamber pressure of $10^{-5}$ torr appears to be an acceptable compromise between reduced background scattering and a smaller collimating-chamber pumping system.

## BEAM CHOPPER AND SPEED SELECTOR

The beam chopper and speed selector, referred to sometimes as "the chopper-selector", serves simultaneously to chop the beam into bursts (thereby facilitating use of the time-of-flight technique), to modulate the beam (thereby facilitating the detection of a beam with density orders of magnitude lower than the density of the residual gas) and to filter out those beam molecules with speeds differing greatly from a selected speed (thereby facilitating interpretation of data). Principal design features of this component, described by Plüe,[37] are reviewed in this section.

Fundamental in the design of the chopper-selector is a measure of the speeds of the molecules which are to be transmitted. A satisfactory measure is provided by the most probable speed in the beam. The speed distribution in a nozzle beam, after passing through both collimating orifices, is given by

$$I(s)ds = \frac{2 s^3 e^{-(s-S)^2} ds}{\sqrt{\pi}\, S\,(1 + \operatorname{erf} S)(S^2 + \frac{3}{2}) + e^{-S^2}(1 + S^2)} \qquad (15)$$

where $I(s)\,ds$ is the molecular flux in speed range $ds$ and $s$ is speed ratio $\equiv u/(2\,kT/m)^{1/2}$. Hence, the most probable speed ratio $\tilde{s}$ in the beam is the speed ratio at which the right-hand side of Equation (15) is a maximum, i.e.,

$$\tilde{s} = \frac{S + (S^2 + 6)^{1/2}}{2} \tag{16}$$

If molecules with this speed ratio are to be transmitted, then the constraint

$$\frac{\Lambda\omega}{U\phi} = \frac{S + (S^2 + 6)^{1/2}}{2S} \tag{17}$$

where $\Lambda$ is distance between entrance and exit sections of rotor, $\omega$ is angular speed of rotor and $\phi$ is relative angular displacement of entrance and exit sections, must be applied to the chopper-selector design. Note that, for $S >> 1$, this constraint simplifies to $\Lambda\omega/U\phi \approx 1$.

A second constraint on the design of the chopper-selector is imposed by the desire for good resolution of the transmitted molecules. Resolution R is defined by

$$R \equiv \frac{s_{max} - s_{min}}{s_\tau} \tag{18}$$

where $s_{max}$ and $s_{min}$ are respectively the maximum and minimum speed ratios of the transmitted molecules and $s_\tau \equiv \Lambda/(\phi/\omega)(2\ kT/m)^{1/2}$ is the speed ratio of those molecules with transit time equal to the delay time of the exit section of the rotor relative to the entrance section. Expressing the right hand side of this expression as a function of geometrical parameters of the rotor is facilitated by an examination of the selector transmission diagram (cf. Figure 6). As a function of transit times,

$$R = \frac{\frac{1}{\tau - \beta} - \frac{1}{\tau + \beta}}{\frac{1}{\tau}} \tag{19}$$

where $\tau \equiv \phi/\omega$ is the delay time of the exit section of the rotor relative to the entrance section, $\beta \equiv \theta/\omega$ is the open time of a typical slit and $\theta$ is the slit-opening angle. Hence, as a function of geometrical parameters of the rotor,

$$R = \frac{2(\theta/\phi)}{1 - (\theta/\phi)^2} \tag{20}$$

Equation (20) indicates that good resolution is obtained at small values of the

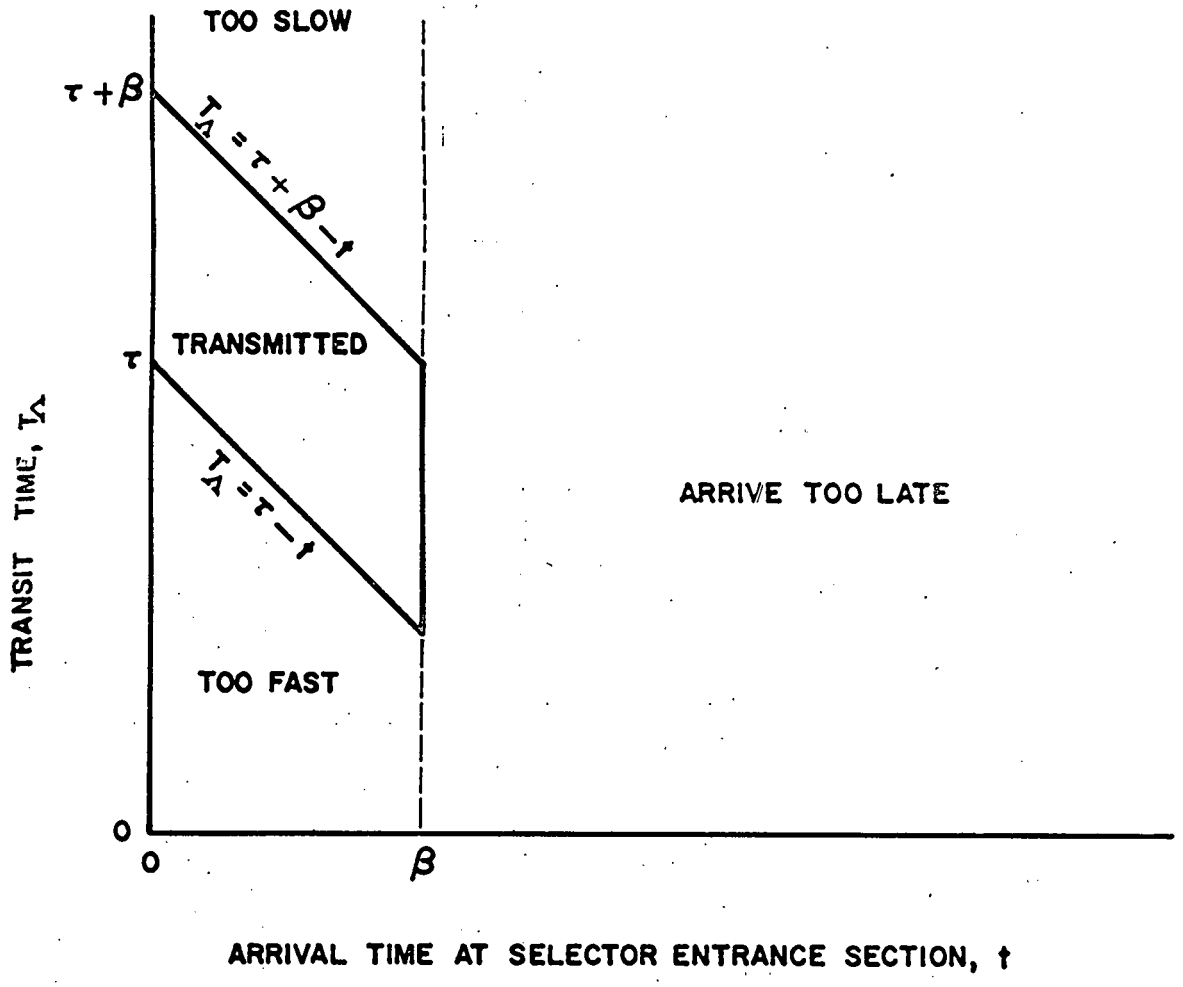


TRANSMISSION DIAGRAM FOR CHOPPER-SELECTOR

FIGURE 6

ratio of the opening angle $\theta$ and the delay angle $\phi$.

A third constraint is imposed by the desire for a high-intensity beam, i.e., for transmission of a large fraction of the molecules admitted to the chopper-selector. The fraction $\mathcal{T}$ of admitted molecules which are transmitted may be written

$$\mathcal{T} = \frac{\int_0^{\beta} dt \int_{\tau-t}^{\tau+\beta-t} I(T_\Lambda) d\, T_\Lambda}{\int_0^{\beta} dt \int_0^{\infty} I(T_\Lambda) d\, T_\Lambda} \tag{21}$$

where $I(T_\Lambda)\, dT_\Lambda$ is the molecular flux in the transit-time range $dT_\Lambda$ and t is time measured from the time of opening of the slit in the entrance section. Reversing the order of integration (cf. Figure 6), one may write

$$\int_0^{\beta} dt \int_{\tau-t}^{\tau+\beta-t} I(T_\Lambda) dT_\Lambda$$

$$= \int_{\tau-\beta}^{\tau} dT_\Lambda \int_{\tau-T_\Lambda}^{\beta} I(T_\Lambda)\, dt + \int_{\tau}^{\tau+\beta} dT_\Lambda \int_0^{\tau+\beta-T_\Lambda} I(T_\Lambda) dt$$

$$= \int_{\tau-\beta}^{\tau} (\beta-\tau+T_\Lambda)\, I(T_\Lambda)\, dT_\Lambda + \int_{\tau}^{\tau+\beta} (\beta+\tau-T_\Lambda) I(T_\Lambda)\, dT_\Lambda$$

so that

$$\mathcal{T} = \frac{\int_{\tau-\beta}^{\tau} (\beta-\tau+T_\Lambda)\, I(T_\Lambda)\, dT_\Lambda + \int_{\tau}^{\tau+\beta} (\beta+\tau-T_\Lambda)\, I(T_\Lambda)\, dT_\Lambda}{\beta \int_0^{\infty} I(T_\Lambda)\, dT_\Lambda} \tag{22}$$

Equation (22) may be written alternatively with speed ratio as variable of integration. Recall that

$$s = \Lambda / T_\Lambda (2kT/m)^{1/2}$$

$$s_{min} = \Lambda / (\tau+\beta)(2kT/m)^{1/2}$$

$$s_\tau = \Lambda / \tau (2kT/m)^{1/2}$$

$$s_{max} = \Lambda / (\tau-\beta)(2kT/m)^{1/2}$$

Hence, Equation (22) may be written

$$\mathcal{T} = \frac{\int_0^\infty \Gamma(s_{min}, s, s_{max})\, I(s)\, ds}{\frac{1}{2}\left(\frac{1}{s_{min}} - \frac{1}{s_{max}}\right) \int_0^\infty I(s)\, ds} \tag{23}$$

where the transmission function $\Gamma(s_{min}, s, s_{max})$ is

$$\begin{aligned} \Gamma(s_{min}, s, s_{max}) &= 0 && s < s_{min} \\ &= \frac{1}{s_{min}} - \frac{1}{s} && s_{min} < s < s_\tau \\ &= \frac{1}{s} - \frac{1}{s_{max}} && s_\tau < s < s_{max} \\ &= 0 && s_{max} < s \end{aligned} \tag{24}$$

A large value of $\mathcal{T}$ is realized if $s_{min} \ll s_\tau \ll s_{max}$, in direct opposition to the conditions necessary for a small value of the resolution R (cf. Equation 18). The speed distribution of the molecules transmitted by the chopper-selector is given by the product of the distribution function for the molecules arriving at the entrance section and the transmission function of Equation (24). (Cf. Figure 7.)

Additional constraints on the design of the chopper-selector are imposed by material properties and fabrication techniques. For example, material properties place an upper limit on the rotor speed whereas fabrication techniques place lower limits on certain dimensions.

Consider now the application of these design constraints to the design of the chopper-selector for the UCLA nozzle beam. Recall that design conditions for this beam include a speed ratio S of 9.13. Hence, from Equation (17),

$$\frac{\Lambda\omega}{U\phi} \approx 1 \tag{25}$$

Choosing R = 1/3, one obtains, from Equation (20),

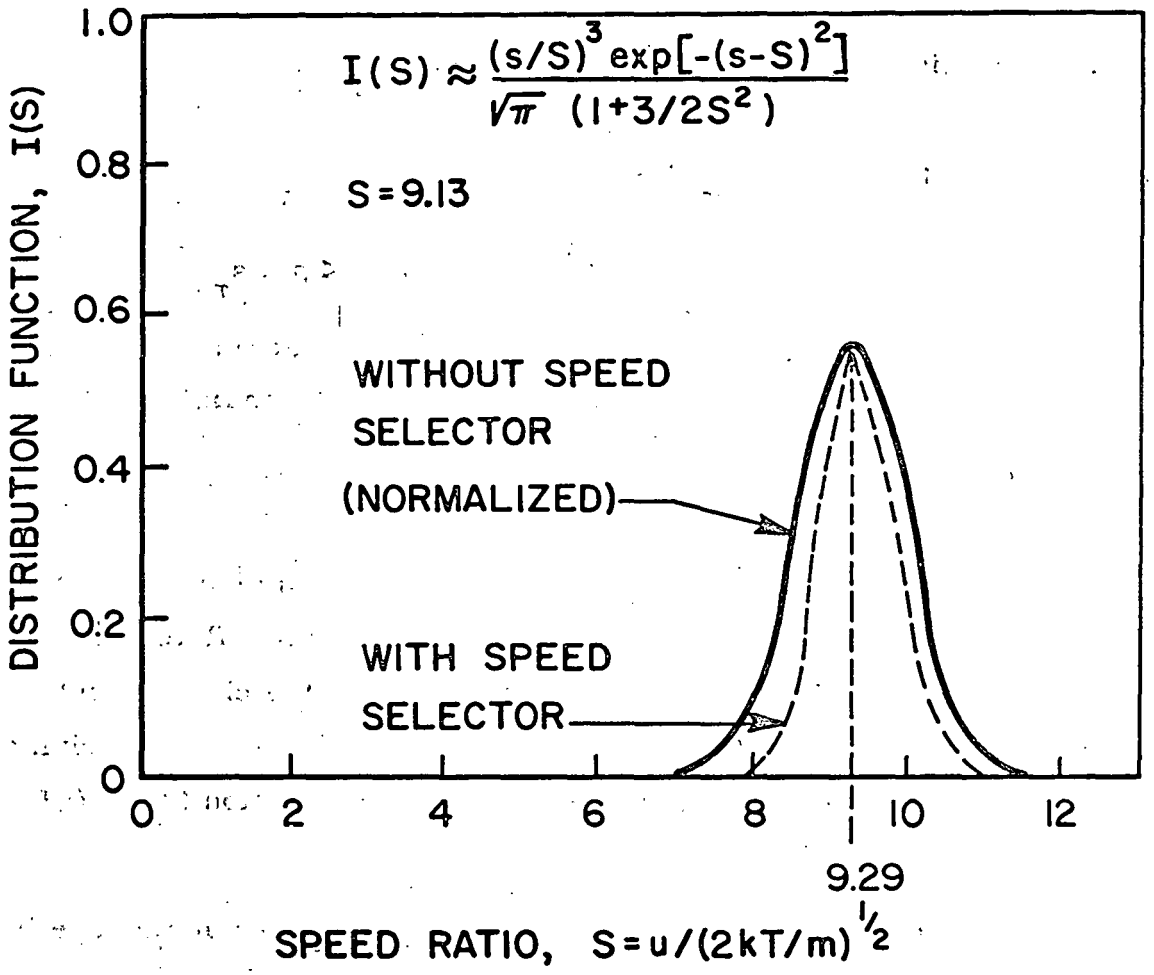


SPEED DISTRIBUTION IN COLLIMATED NOZZLE BEAM
(Ref. 37, Figure 23)

FIGURE 7

$$\frac{\theta}{\phi} \approx \frac{1}{6} \qquad (26)$$

Setting $s_\tau = \tilde{s}$, $s_{max}/s_\tau \; [= \phi/(\phi-\theta)] = 6/5$, $s_{min}/s_\tau [= \phi/(\phi+\theta)] = 6/7$, and

$I(s) = \frac{(s/S)^3 \exp[-(s-S)^2]}{\pi^{1/2}(1+3/2\,S^2)}$ (cf. Equation 15, $S >> 1$), with $\tilde{s} = 9.29$ (cf. Equation 16, $S = 9.13$), one obtains, using Equation (24), the speed distribution of the transmitted molecules shown by the dotted curve in Figure 7 and, from Equation (23), a transmission $\mathcal{T}$ of 0.64. Considerations of rotor stresses due to centrifugal forces motivated the selection of aluminum alloy 7075-T6, a radius of 10 cm, and a maximum speed of 25,000 rpm for the rotor. The slit-opening angle $\theta$ must be large enough so that it can be machined conveniently but not so large that the rotor length is excessive (cf. Equations 25 and 26). An angle of two degrees appears to meet these requirements. Then, from Equation (26), the phase angle $\phi$ is twelve degrees; from Equation (25), for $\omega$ = 10,000 rpm at U = 2400 m/sec, the rotor length $\Lambda$ is 0.5 m. Note that, at the maximum speed of 25,000 rpm, this rotor would pass molecules with speeds in the neighborhood of 6,000 m/sec.

Speed-selector types examined in the search for a type suitable for the present system (requiring a chopped, modulated speed-filtered beam) included the phase-shift selector,[52-53] the multi-disk selector (e.g., References 54-57) and the helical selector.[58-60] Considering such factors as fabrication, alignment, transmission, resolution, transmission of side-bands, driving torque and stability, a two-disk chopper-selector with two slits in each disk was selected. Principal characteristics of the final design are tabulated in Table IV; a photograph of the fabricated chopper-selector is included as Figure 8.

A wide continuous range of rotor speeds is available through use of an air-turbine drive; speed of the turbine rotor is regulated by a cartesian manostat; speed of the chopper-selector rotor is monitored by an optical tachometer and a decade counter. The need for a rotating seal is obviated by transmitting torque from the turbine to the chopper-selector by permanent magnets rotating on both sides of a non-ferrous insert in the vacuum-chamber

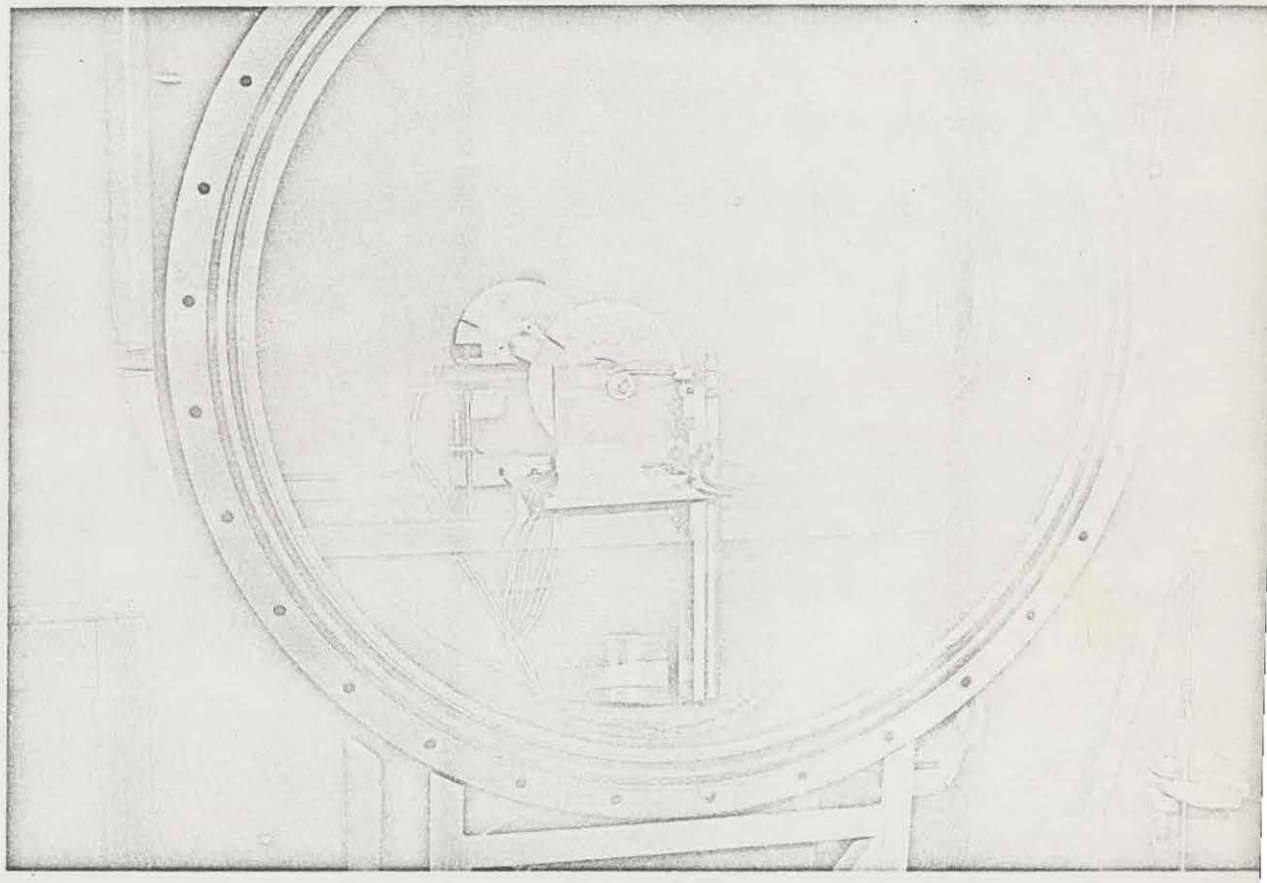

BEAM CHOPPER AND SPEED SELECTOR
(Ref. 37, Figure 13. Vertical drive shaft shown here has been replaced by horizontal drive shaft)

FIGURE 8

wall (cf. Figure 1). Those bearings located within the vacuum chamber are Barden 100T precision ball bearings lubricated with General Electric F50 silicone oil. The chopper-selector is located in the detection chamber since location in the collimating chamber is precluded by the presence of either the sorption pump or the turbo pump in that chamber.

TABLE IV

PRINCIPAL CHARACTERISTICS OF CHOPPER-SELECTOR

| | |
|---|---|
| Number of Disks | 2 |
| Number of Slits Per Disk | 2 |
| Disk Radius | 10 cm |
| Distance Between Disks | 50 cm |
| Slit Angle | $2^{o}$ |
| Phase Angle | $12^{o}$ |
| Maximum Rotational Speed | 25,000 rpm |
| Maximum Transmitted Speed | 6,000 m/sec |
| Resolution, R | 0.33 |
| Transmission, $\mathcal{T}$ | 0.64 |

The chopper-selector has been operated routinely at speeds up to 4600 rpm in detector calibrations. Attempts to attain higher speeds have been held in abeyance pending completion of these calibrations.*

## BEAM DETECTOR

The beam source, collimator and chopper-selector have been described in preceding sections of this paper. In the present section, the time-of-flight technique (used for measuring molecular speeds) and the beam detector are described.

Examine first the possible speed range of particles arriving at the detector (subsequent to scattering by the target) at time $t_d$, where t is time measured from the time of opening of the slit in the exit section of the

*See Note Added in Proofreading, p. iii.

chopper-selector. (Cf. Reference 36.) The first molecules leaving this exit section have a speed range

$$\frac{\Lambda}{\tau} \leq u \leq \frac{\Lambda}{\tau-\beta} \tag{27}$$

whereas the last molecules leaving have a speed range

$$\frac{\Lambda}{\tau+\beta} \leq u \leq \frac{\Lambda}{\tau} \tag{28}$$

where u is molecular speed. The first molecules to arrive at the target arrive at time

$$t = \frac{L_{st}}{\Lambda/(\tau-\beta)} \tag{29}$$

whereas the last molecules arrive at time

$$t = \beta + \frac{L_{st}}{\Lambda/(\tau+\beta)} \tag{30}$$

where $L_{st}$ is distance from the exit section of the chopper-selector to the target. If the stay times of the molecules on the target are negligible in comparison to the flight times, then molecules arriving at the detector at time $t_d$ have target-detector flight times in the range

$$t_d - \beta - \frac{L_{st}}{\Lambda/(\tau+\beta)} \leq t_d - t_t \leq t_d - \frac{L_{st}}{\Lambda/(\tau-\beta)} \tag{31}$$

and speeds in the range

$$\frac{L_{td}}{t_d - \frac{L_{st}}{\Lambda/(\tau-\beta)}} \leq u \leq \frac{L_{td}}{t_d - \beta - \frac{L_{st}}{\Lambda/(\tau+\beta)}} \tag{32}$$

or, in terms of geometrical parameters,

$$\frac{L_{td}}{t_d - L_{st}(\phi-\theta)/\Lambda\omega} \leq u \leq \frac{L_{td}}{t_d - \theta/\omega - L_{st}(\phi+\theta)/\Lambda\omega} \tag{32a}$$

where $t_t$ is arrival time at the target and $L_{td}$ is distance from the target to the detector. To facilitate data interpretation, this speed range must be small. It is plotted in Figure 9 as a function of arrival time at the detector for design conditions of the beam, i.e., for $L_{td} = 0.2$ m, $L_{st} = 0.3$ m, $\Lambda = 0.5$ m, $\phi = 12^{\circ}$, $\theta = 2^{\circ}$, and $\omega = 10,000$ rpm. It is seen that the possible speed range is small for thermal speeds (complete accommodation) but large for speeds of the order of 2400 m/sec (no accommodation). For a given chopper-selector length $\Lambda$, the possible speed range is decreased if $\theta/\phi$ is decreased (i.e., if the resolution R is improved), if the length $L_{st}$ is decreased, or if the length $L_{td}$ is increased.

Consider now the problem of determining the speed distribution of a reflected beam given the outputs of a photocell located at the second disk of the chopper-selector and of a through-flow ionization detector located in the path of the reflected beam (cf. Figures 1 and 10). If the possible speed range is small, then one may treat the molecules from one burst as though they all leave the target simultaneously and the computations are simplified greatly; the intensity (time-dependent) is given by

$$I_d(t_d) = - \frac{N F(u) u^2 du}{L_{td}^2 dt_d} \tag{33}$$

where N is the total number of molecules in the burst, F(u) is the velocity-distribution function (the fraction of molecules in unit volume of velocity space), $u^2 d\Omega du$ is a differential volume in velocity space, $L_{td}^2 d\Omega$ is a differential area in physical space, $\Omega$ is solid angle, u is speed, and $dt_d$ is the time required for molecules in speed range -du to pass through the detector. Since speed u is related to time-of-flight $T_{td} \equiv t_d - t_t$ by

$$u = \frac{L_{td}}{T_{td}} \tag{34}$$

one may write

$$- \frac{du}{dt_d} = - \frac{du}{dT_{td}} = \frac{L_{td}}{T_{td}^2} \tag{35}$$

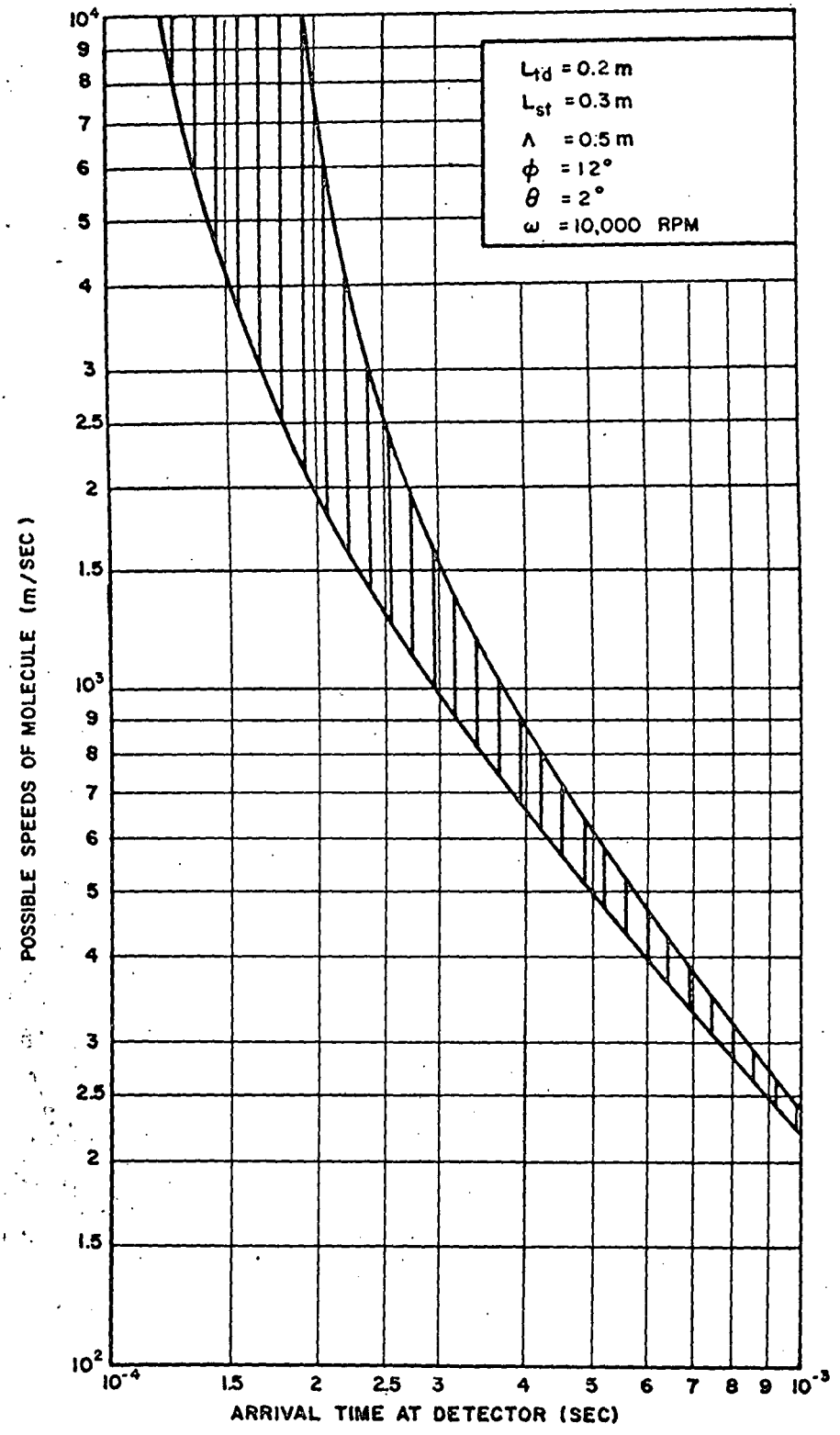


POSSIBLE SPEEDS OF MOLECULES ARRIVING AT DETECTOR AS FUNCTION OF TIME SINCE TIME OF OPENING OF EXIT SECTION OF CHOPPER-SELECTOR

FIGURE 9

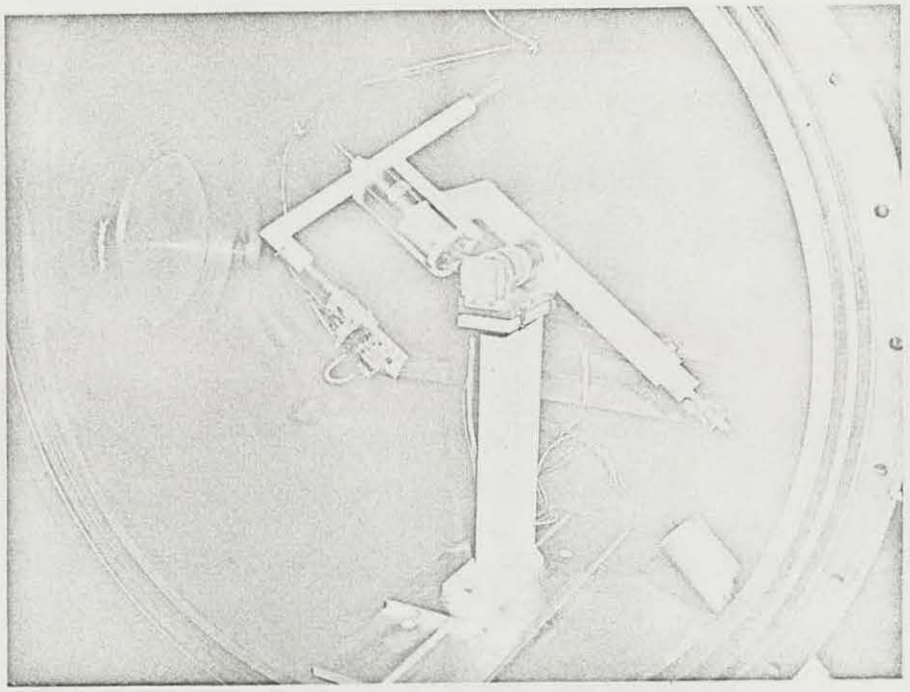

DETECTOR POSITIONING MECHANISM
(Ref. 36, Figure 16)

FIGURE 10

so that

$$I_d(T_{td}) = \frac{N\,F(u)\,u^2}{L_{td}\,T_{td}^2} \tag{36}$$

Since the output of an ionization detector is proportional to the number density $n_d(T_{td})$ of molecules in the detector, substitute $n_d(T_{td})$ for $I_d(T_{td})/u$ and rearrange to obtain

$$F(u) = \frac{T_{td}^3}{N}\, n_d(T_{td}) \tag{37}$$

Finally, defining the calibration constant K by

$$V_d(T_{td}) \equiv K\, n_d(T_{td}) \tag{38}$$

where $V_d(T_{td})$ is the detector output potential, one may write

$$F(u) = \frac{T_{td}^3}{N}\,\frac{V_d(T_{td})}{K} \tag{39}$$

so that the speed distribution F(u) is given, for the case in which the possible speed range is small, by $T_{td}^3\, V_d(T_{td})/NK$ as a function of $L_{td}/T_{td}$. The more complicated case in which the possible speed range is not small is examined briefly in Reference 36. An alternative method of determining the speed distribution using two detectors in series is mentioned in a later paragraph.

The detector (Figure 11 and Reference 42) is a modification of the through-flow, hot-cathode, ionization detector used by Becker et al.[12] It consists essentially of a cathode, anode and ion collector. Ions, produced by bombardment of molecules by electrons accelerating from the cathode to the anode, are attracted to the ion collector and neutralized. The potential drop caused by flow of the neutralizing electrons through a resistor in series with the ion collector is amplified and displayed on an oscilloscope (Figure 12). This potential drop is the detector output potential $V_d(T_{td})$ referred to in the preceding paragraph. See Table V for a comparisc of the principal design features of several beam detectors employing ionizatic of beam molecules by accelerated electrons.

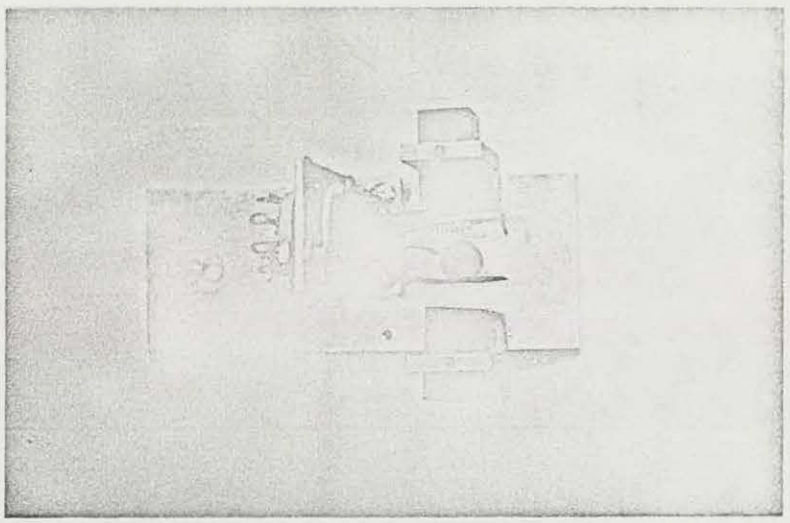

THROUGH-FLOW HOT-CATHODE IONIZATION DETECTOR

FIGURE 11

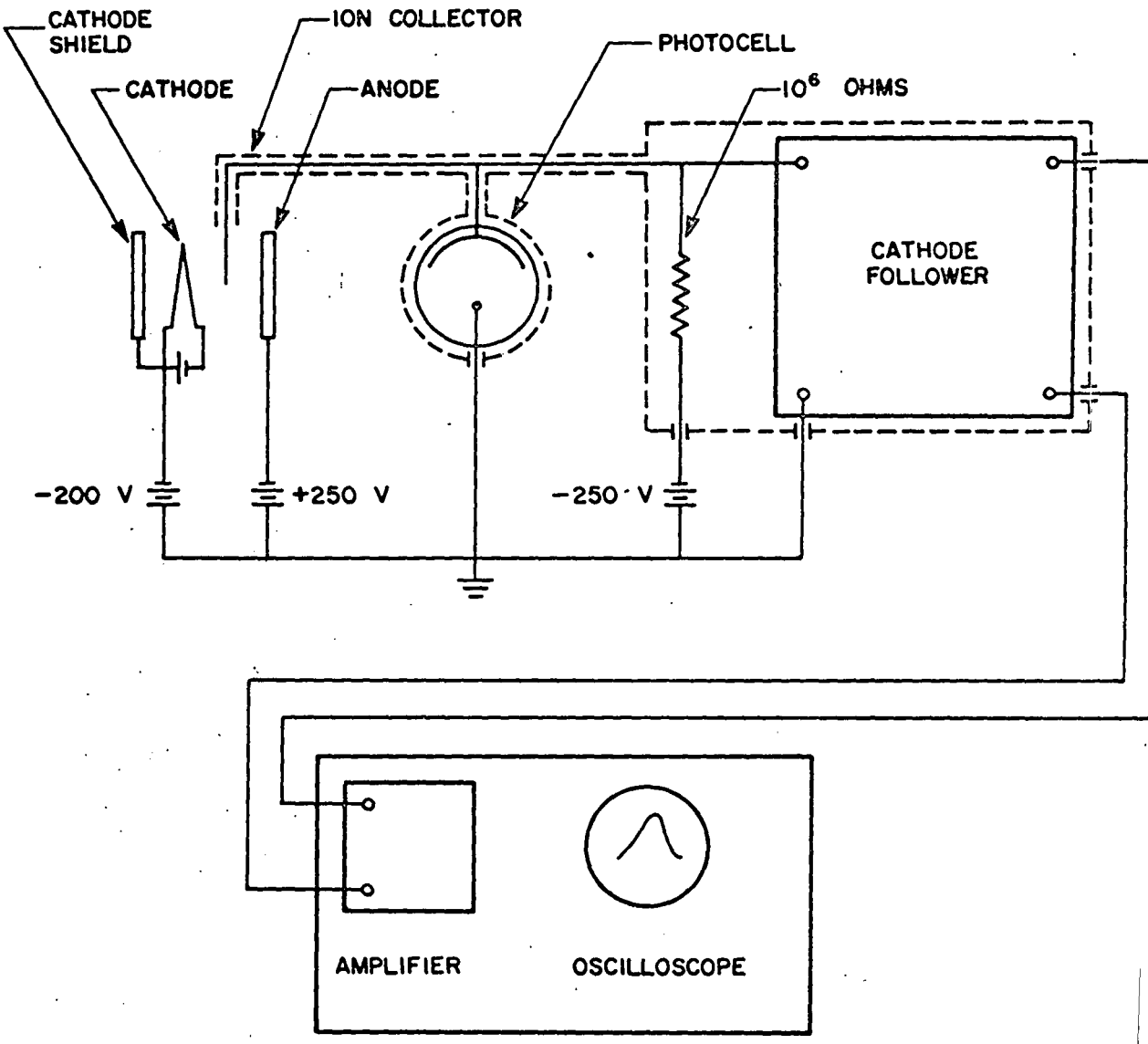


SCHEMATIC DIAGRAM OF DETECTOR AND INDICATING INSTRUMENTS

FIGURE 12

TABLE V

PRINCIPAL DESIGN FEATURES OF SEVERAL IONIZATION DETECTORS

| Electron Source | Magnetic Field (gauss) | Fraction Ionized | Detector | Beam Intensity $\left(\frac{\text{molecules}}{\text{cm}^2\,\text{sec}}\right)$ | Beam Density $\left(\frac{\text{molecules}}{\text{cm}^3}\right)$ | Reference |
|---|---|---|---|---|---|---|
| 2 transverse opposing cathodes | A few hundred | $\frac{1}{3000}$ | Electron multiplier | | | 61 |
| 2 parallel opposing cathodes | 200 | $\frac{1}{20}$ | Electron multiplier | | $1\times10^{5}$ | 62 |
| Electron gun | | $\frac{1}{100}$ | Electron multiplier | | $3\times10^{4}$ | 63 |
| 1 parallel cathode | None | $\frac{1}{30}$ | Ion Collector | $1.4\times10^{10}$ | $2\times10^{5}$ | 64 |
| 1 transverse cathode | Unknown strength | Small | Ion Collector | | | 12 |
| Electron gun | | $\frac{1}{40}$ | Electron multiplier | $6\times10^{9}$ | | 65 |
| 1 cathode crossing beam | None | $\frac{1}{400}$ | Electron multiplier | $1.8\times10^{8}$ | $4\times10^{3}$ | 66 |
| 1 transverse cathode | 150 | $\frac{1}{7000}$ | Ion Collector | $1.5\times10^{14}$ | $3.2\times10^{9}$ | this paper |

NOTES:

1. All sources employ heated tungsten cathodes.
2. Unless indicated otherwise, all cathodes are located outside beam.
3. All beams are modulated to facilitate separation of beam effects from background effects.

As a compromise between high resolution and high detector output, a detector opening diameter of 1.27 cm was selected. (Recall that the target-detector distance is 0.2 m.) Calculations[42] of trajectories of ions in electrostatic fields indicate that, neglecting effects of cathode and anode potentials, all argon ions with energies less than 1.2 ev and with straight-line extensions of initial flight paths passing within 0.64 cm of the center of the collector are collected by a spherical ion collector with radius of 0.04 cm and potential of -300 volts. Taking into account the detrimental effects of a cathode at negative potential and the beneficial effects of using a cylindrical collector (with axis parallel to the initial ion flight paths), a cylindrical geometry and a potential of -250 volts were selected. In order to avoid the problems of poisoning upon exposure to atmospheric oxygen (encountered with oxide-coated cathodes), a tungsten cathode (with surface area of 0.8 $cm^2$ and operatin temperature of 2500°K) was chosen. In order to produce an ion current which can be detected with available instruments, a cathode-anode electron current of the order of $10^{-2}$ ampere is required. Taking into account the fact that this electron current is space-charge limited, the Langmuir-Child Law predicts that, for plates with areas of 0.8 $cm^2$ each and separated by a distance of 1.27 cm, a potential of approximately 400 volts is required to produce the required value of this current. Considering that the ion collector (at -250 volts) is located between the cathode and anode, a cathode-anode potential of 450 volts, with the cathode at -200 volts and the anode at +250 volts, was selected. A temperature-limited electron current of 0.007 ampere was measured in the completed detector.

A cathode shield, at the same potential as the cathode, reduces electr losses to the side of the cathode facing away from the anode. Permanent magnets focus the electrons accelerating from the cathode to the anode - reducing spreading due to mutual repulsions and random motions. A field strength of 150 gauss results in a Larmor radius of 0.02 cm for electrons with speed perpendicular to the magnetic field corresponding to an energy of 1 ev. (The same field strength results in a Larmor radius of 6 cm for argon ions with an energy of 1 ev, i.e., it has a negligible effect on the ion-collecti

process.) In order to reduce the collection of ions by the cathode, the upstream end of the ion collector is located approximately in the plane of the electron paths.

The molecular intensity, flow rate and density anticipated at the detector in a typical application are included in Table III. For these conditions and an ionization probability of 0.4 (Reference 67, Figure 18), approximately one molecule in $7 \times 10^3$ molecules is ionized, i.e., a negligible fraction of the beam is removed by the detector. Hence, several detectors of this type may be used to monitor simultaneously the beam at several points along the beam path, thereby providing a method for making time-of-flight measurements alternative to (and perhaps more versatile and accurate than) the method using a photocell and one detector described earlier.

For the calibration tests described in the next paragraph, the detector output was amplified and displayed using a cathode follower of the type developed by Hagena and Henkes,[12] a Tektronix Type L amplifier and a Tektronix RM 45 oscilloscope. (Cf. Figure 12.) Addition of a preamplifier might facilitate the detection of weaker beams. Stability was improved (and power-supply noise reduced) by using direct-current power supplies for the cathode, cathode heater, anode and ion collector; since stability of the ion-collector potential is specially important, a battery was used for the ion collector. External noise was reduced by shielding the appropriate leads and components (cf. Figure 12).

The detector has been calibrated in effusive flows from the collimating chamber into the detecting chamber chopped by the first disk of the chopper-selector. A typical oscilloscope trace photographed during these calibration tests is reproduced as Figure 13; a plot of detector output as a function of density of effused molecules at the detector is given in Figure 14. Densities lower than $3 \times 10^9$ molecules/cm$^3$ were not detectable due to lack of a preamplifier. From Figure 14, a calibration constant K of $6.7 \times 10^{-10}$ mv per molecule/cm$^3$ is computed. This value is approximately 1/4 the value one would predict for an ionization probability of 0.4 and collection of all ions. Considering the complex nature of the potential field in the detector and the

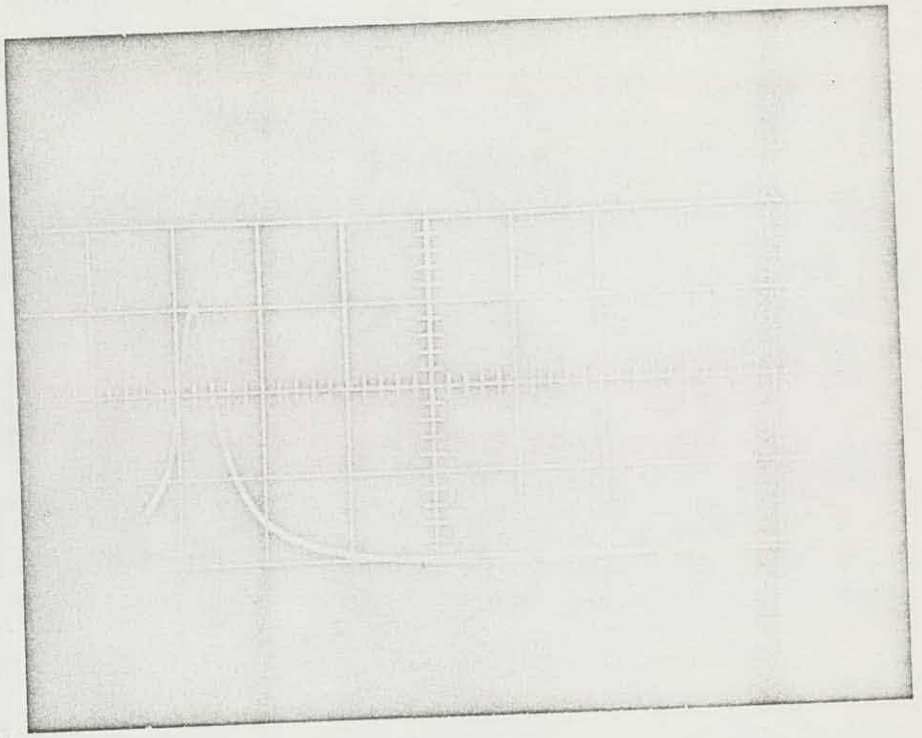

OUTPUT FROM DETECTOR AS DISPLAYED
ON OSCILLOSCOPE SCREEN
(Ref. 42, Figure 20. Vertical axis - 0.02 volt/cm; horizontal axis - 0.0005 sec/cm, source pressure - 0.01 torr, equivalent to $1.72 \times 10^{11}$ atoms argon/$cm^3$ at detector)

FIGURE 13

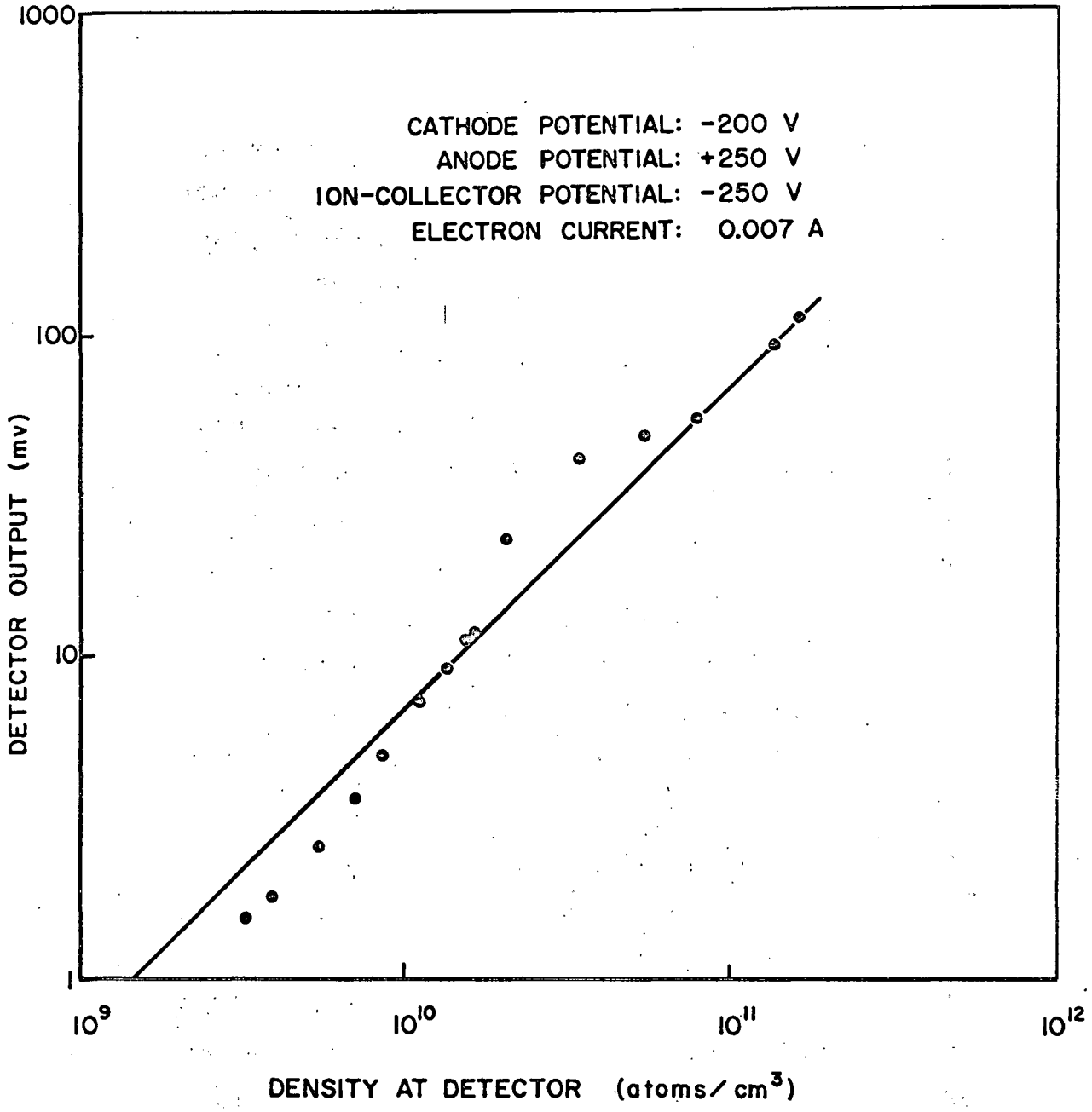


DETECTOR CALIBRATION CURVE OBTAINED WITH CHOPPED EFFUSIVE FLOW OF ARGON
(Ref. 42, Figure 23)

FIGURE 14

simple models used in the calculations, this deviation from the predicted value is not surprising.*

The lowest detected flow density was two orders of magnitude lower than the background density. As mentioned previously, it is anticipated that addition of a preamplifier would facilitate detecting flow densities lower than the lowest density listed in Table III. Support for this anticipation is provided by the beam densities listed for the several ionization detectors reviewed in Table V. Beam detection under such conditions is made possible by use of a modulated beam and an alternating-current amplifier.

## VACUUM PUMPS

As indicated in the section titled Principal Design Features, UCLA Nozzle Beam and in Figure 1, the vacuum system is divided into three chambers - a source chamber, a collimating chamber and a detecting chamber each with its own pumping system. If the maximum allowable pressures for the three chambers differ significantly from each other, then the use of three different pumping systems minimizes the required pumping capacity. The several pumping systems (including two novel vacuum pumps developed in the UCLA Molecular-Beam Laboratory) used in this facility are described in the present section.

Consider first the pumping system for the source chamber. As indicated in the section titled Beam Source and in Figures 2 and 3, the source-chamber pumping system must remove 99 gms of argon per hour either at 2 torr (if the converging-diverging nozzle and hypersonic diffuser are used) or at $10^{-2}$ torr (if the converging nozzle and free jet are used). Hence, in terms of volume-flow rates at $300^{\circ}$K, this pumping system must remove either 6 $\ell$/sec at 2 torr or $1.3 \times 10^{3}$ $\ell$/sec at $10^{-2}$ torr. These pumping capacities are provided respectively by a Stokes Model 212-H Microvac Pump (66 $\ell$/sec displacement) and by a 16-inch Stokes Series 150 Ring-Jet Booster Pump ($4.5 \times 10^{3}$ $\ell$/sec maximum pumping speed).

*See Note Added in Proofreading, p. iii.

Consider now the collimating chamber. Since the removal of molecules by flow through the collimating orifice is negligible in comparison with the addition of molecules by flow through the skimmer orifice, steady-state operation requires that approximately $10^{19}$ molecules per second (cf. Table III) be removed by the pumping system. In order to realize beam attenuations of the order of (or less than) 10%, a molecular density of the order of or less than $3 \times 10^{11}$ molecules/cm$^3$ must be maintained (cf. section titled Beam Collimator). Hence, a pumping system with a speed of the order of (or greater than) $3 \times 10^4$ $\ell$/sec is required. Pumping systems which were considered include diffusion pumps, cryogenic pumps, sorption pumps and turbo pumps. If baffled oil-diffusion pumps were used, then at least one (perhaps two) 32-inch diffusion pump would be required; it was eliminated from consideration by its high initial cost relative to total grant funds and by its bulk. Cryogenic pumps were eliminated either due to high operating costs (in the case of liquid helium or liquid neon) or due to high explosion hazards (in the case of liquid hydrogen). Preliminary calculations revealed, however, that either a sorption pump cooled with relatively inexpensive liquid nitrogen or a two-stage radial-flow turbo pump might have the required pumping speed as well as modest initial and operating costs. Hence, development programs for the two latter pumping systems were initiated simultaneously, the sorption-pump program[34, 39] funded by NSF Grant G-9783 and the turbo-pump program[41] by UCLA Grant 1804.

An examination of available data on sorption of gases at low pressures (e.g., References 68-72) led to the decision to use either a charcoal or a zeolite in the sorption pump and to base the final selection on a preliminary study of sorption characteristics of representative samples (Barnebey-Cheney AC-4 coconut-shell charcoal and Linde 13x molecular sieve) of these two sorbents. From nitrogen sorption isotherms at 77°K and relatively high pressures (Figure 15), surface areas of 1300 m$^2$/gm and 740 m$^2$/gm were computed respectively for the activated charcoal and for the molecular sieve; argon sorption isotherms at 77°K and relatively low pressures (Figure 16) indicate that, at 77°K and in the neighborhood of $10^{-5}$ torr, Barnebey-Cheney AC-4

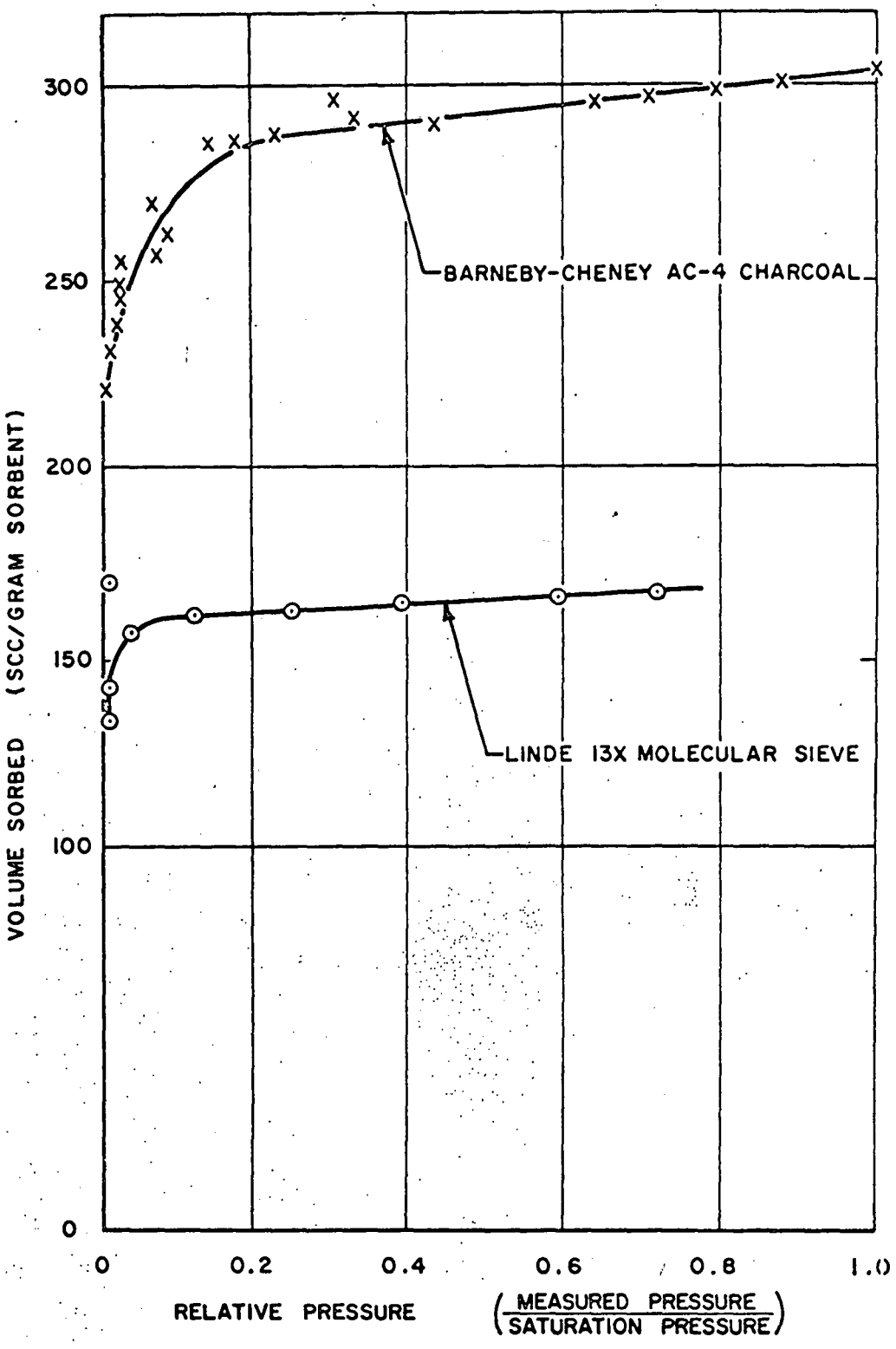


NITROGEN SORPTION ISOTHERMS AT 77° K
(Ref. 34, Figure 1)

FIGURE 15

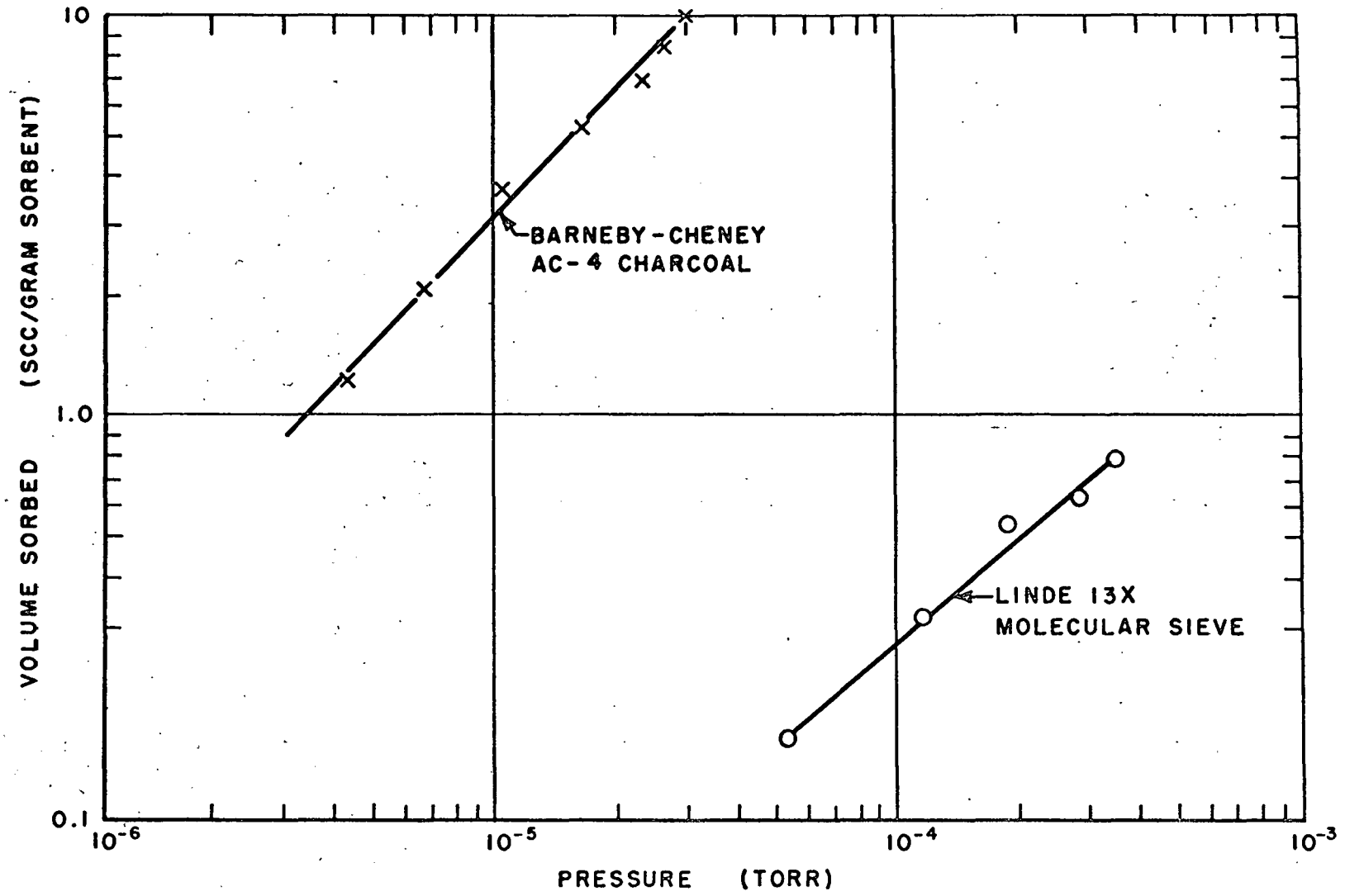


ARGON SORPTION ISOTHERMS AT 77°K AND LOW PRESSURES
(Ref. 34, Figure 3)

FIGURE 16

activated charcoal sorbs at least an order of magnitude more argon than does Linde 13x molecular sieve. Charcoals have the additional advantage, relative to zeolites, of a high thermal conductivity, facilitating heating during the desorption process and cooling during the sorption process. Hence, Barnebey-Cheney AC-4 activated charcoal was selected for use in the sorption pump. Once the sorbent and sorbate are selected, the key parameters in the design of a sorption pump are (a) the area of the sorbent bed exposed to the gas being pumped (related to the pump speed) and (b) the quantity of sorbent in the pump (related to the pump endurance). For the case in which the temperature of the gas being pumped is equal to the temperature of the sorbent surface and the molecular speed distribution is Maxwellian, the required surface area A of the sorbent bed is given, according to the kinetic theory of gases by

$$A = \frac{\dot{N}(2\pi mkT_c)^{1/2}}{\alpha (p_c - p_{eq})} \tag{40}$$

where A is area of sorbent bed exposed to gas being pumped, N is flow rate of molecules, $\alpha$ is a sticking coefficient (equal to or less than unity), $p_c$ is pressure in chamber and $p_{eq}$ is equilibrium pressure in chamber for given sorbent temperature and for given quantity of sorbate sorbed. The required quantity of sorbent may be calculated using the data of Figure 16. If the sticking coefficient is unity and if the equilibrium pressure is zero, then, for a flow rate of $10^{19}$ molecules/second, a density of $3 \times 10^{11}$ molecules/cm$^3$ and a gas temperature of 100°K, Equation (40) indicates that an area of 0.6 m$^2$ is required. Since, in practice, the sticking coefficient is less than unity and the equilibrium pressure is greater than zero, the required area will be perhaps appreciably greater than this calculated lower limit. For a chamber pressure of $3 \times 10^{-6}$ torr, Figure 16 indicates that Barnebey-Cheney AC-4 activated charcoal can sorb approximately 0.8 scc argon per gram sorbent so that, for a flow of $10^{19}$ argon atoms per second for 8 hours, 13 kilograms of charcoal are required. Since, in practice, the charcoal temperature may be higher than 77°K and the desorption may not be as complete as for the data of Figure 16, the required quantity will be perhaps appreciably greater than this calculated lower limit.

Beginning with these calculated minimum values of sorbent-bed surface area and sorbent quantity, the sorption pump shown photographically in Figure 17 and schematically in Figure 18 was designed, built and tested. This pump contained approximately 15 kilograms of Barnebey-Cheney AC-4 activated charcoal in a bed with surface area of approximately 1.9 $m^2$. After activating the charcoal, by desorbing at 325°C and cooling to 100°K (requiring several days), argon was leaked into the pump and the performance recorded in Figure 19 was measured. (See References 34 and 39 for more detailed descriptions of pump design, activation and performance.) The pump speed decreased from an initial value of approximately 11,000 $\ell$/sec at 100°K to a final value of approximately 9,000 $\ell$/sec at 100°K. By increasing the area of the charcoal bed from 1.9 to 2.85 $m^2$ and by reducing the equilibrium pressure of the system (through a more complete desorption and a reduction of the temperature of the surface of the sorbent bed), it is anticipated that the pumping speed could be doubled (i.e., increased to approximately 20,000 $\ell$/sec at 100°K). This performance is of the order of magnitude required for the collimating-chamber pumping system.

Turbo pumps have been used in vacuum systems only recently - the application to vacuum systems being delayed perhaps by the fact that, in continuum flows, the pressure ratio per stage is relatively small. Recent experimental studies by Becker[73] and Hablanian,[74] as well as analytical and experimental studies by Kruger, Maulbetsch and Shapiro[75-77] have shown that, in free-molecule flows, the pressure ratio per stage is relatively large. These several investigators considered, however, only axial-flow turbo pumps; the volumetric pumping rate, proportional to the frontal area of the annulas containing the blades, is necessarily relatively small. (The axial-flow turbo pump marketed by Arthur Pfeiffer Gmbh of Wetzlar, Germany and by Welch Scientific Company of Chicago, Illinois pumps only 140 $\ell$/sec.) In the study described here, the radial-flow design is considered; the pumping rate, proportional to the area of the cylindrical surface containing the blades, can be relatively large. (The radial-flow turbo pump described here has a calculated

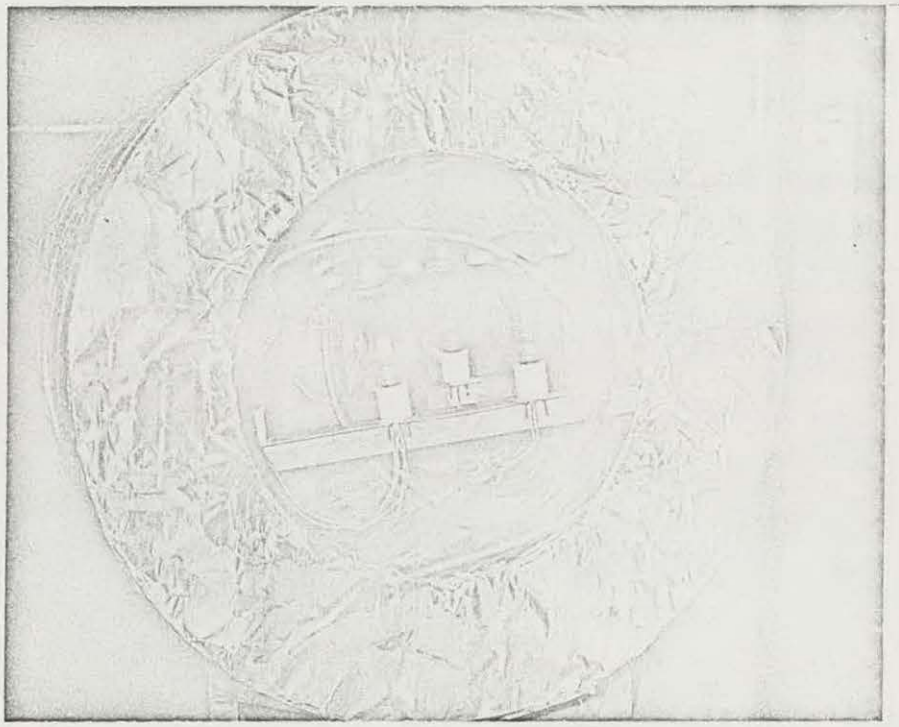

FRONT VIEW OF SORPTION PUMP
(Ref. 34, Figure 4)

FIGURE 17

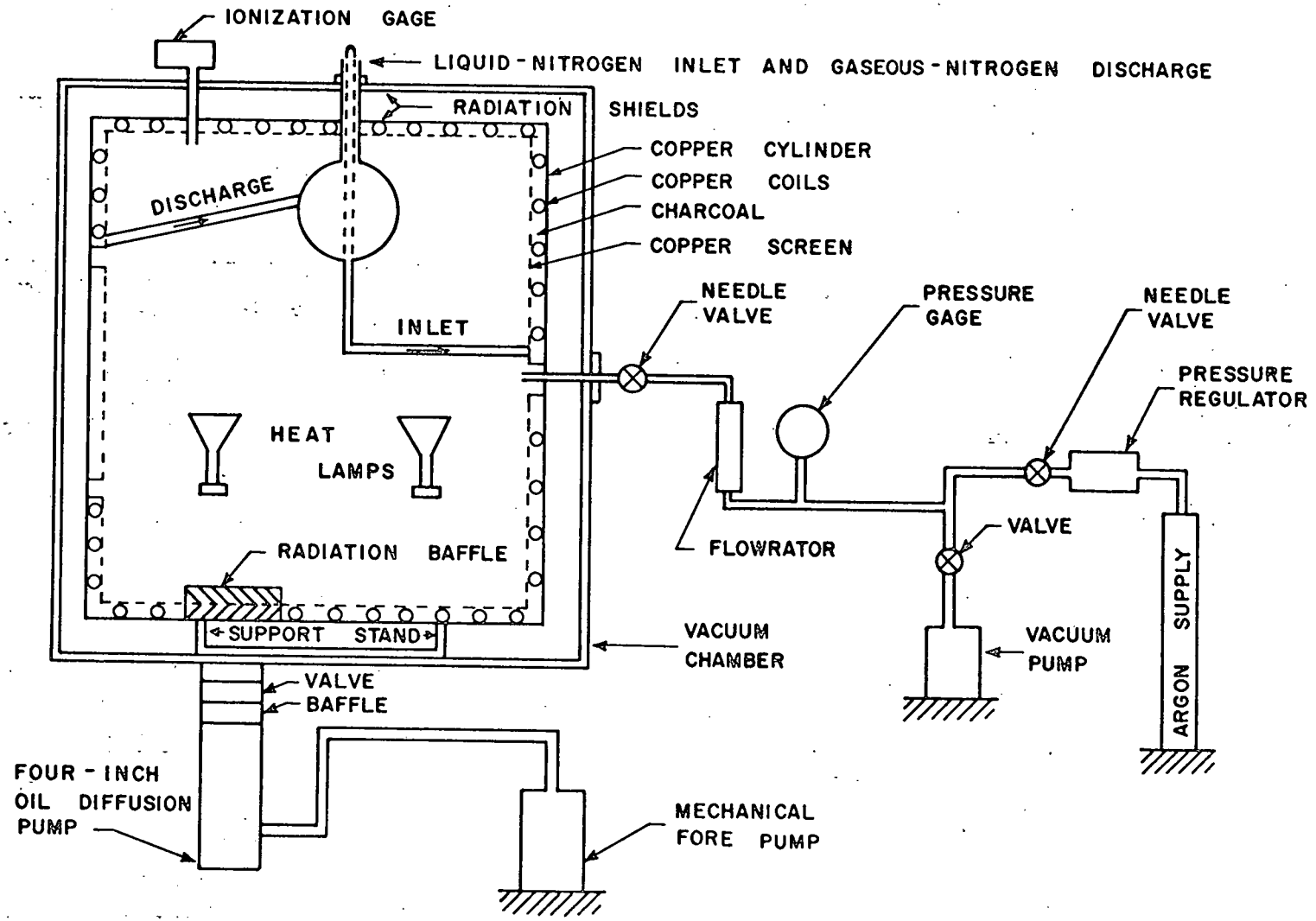


SCHEMATIC DIAGRAM OF SORPTION-PUMP TEST CONFIGURATION
(Ref. 34, Figure 5)

FIGURE 18

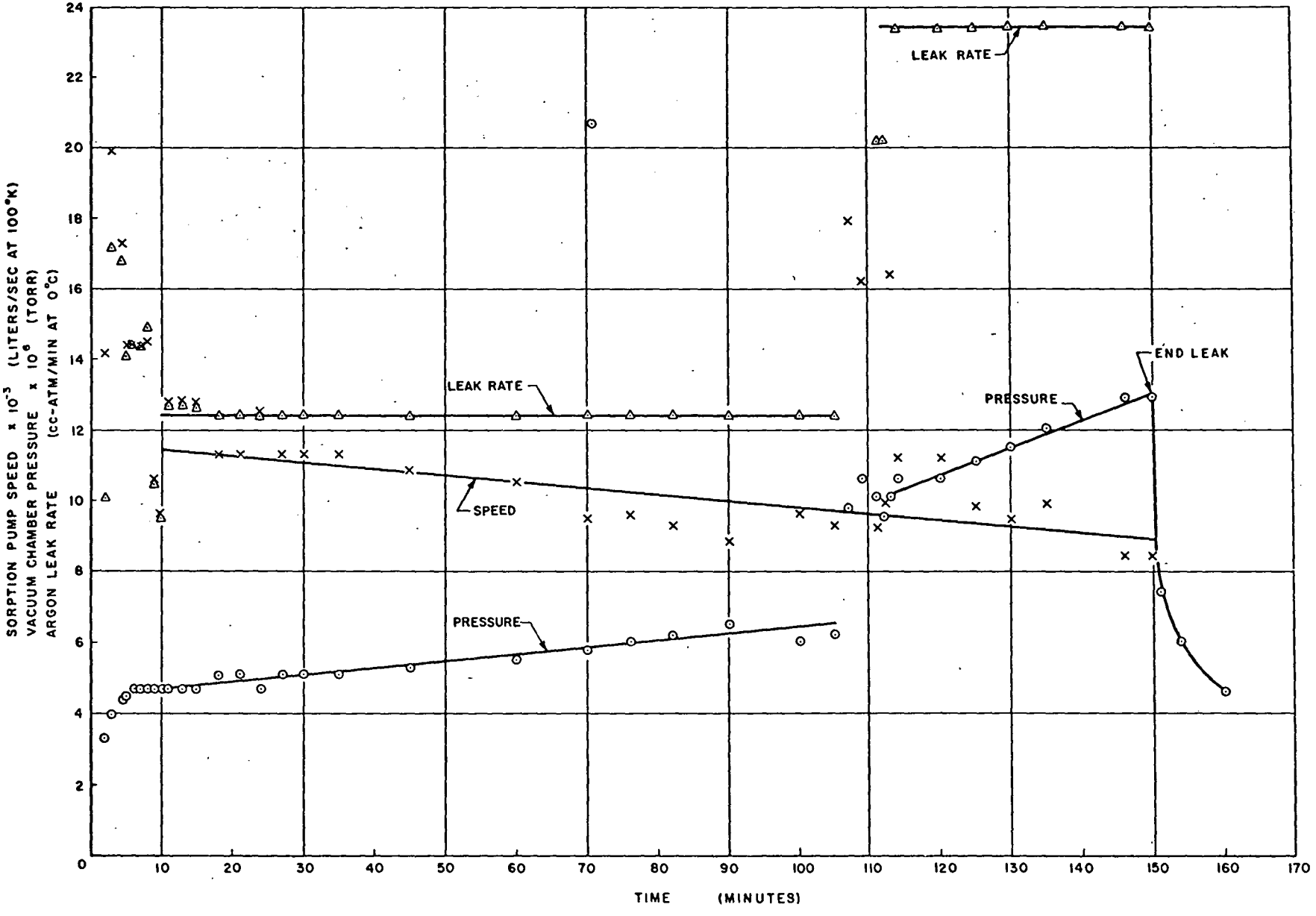


SORPTION-PUMP PERFORMANCE
(Ref. 34, Figure 6)

peak pumping rate of the order of $10^5$ $\ell$/sec.) The molecular pumping rate may be written as a product of through-flow ratio W, molecular incidence intensity G and surface area A, i.e.,

$$\dot{N} = WGA \tag{41}$$

If the molecular speed distributions are Maxwellian, then $G = n_c(8kT_c/\pi m)^{1/2}/4$ so that the required surface area is given by

$$A = \frac{\dot{N}(2\pi mkT_c)^{1/2}}{W p_c} \tag{41a}$$

[Compare Equation (41a), written for the turbo pump, with Equation (40), written for the sorption pump.] If the through-flow ratio is unity, then, for a flow rate of $10^{19}$ molecules/second, a density of $3\times10^{11}$ molecules/cm$^3$ and a gas temperature of 300°K, Equation (41a) indicates that an area of 0.33 m$^2$ is required. Since, in practice, the through-flow ratio is less than unity, the required area will be perhaps appreciably greater than this calculated lower limit. Influenced by the geometry of the existing collimating chamber, an area of 1.37 m$^2$ was selected, requiring a through-flow ratio equal to or greater than 0.24. Keeping in mind this constraint (as well as constraints imposed by material properties and fabrication techniques) and using transmission probabilities calculated by Kruger and Shapiro [cf. Figure 2 and Equation (9) and (10) of Reference 76], the two-stage radial-flow turbo pump characterized in Table VI and shown in Figure 20 was designed, fabricated and tested. The rotor is driven by two 5-horsepower, 440-volt, 3-phase, 3450-rpm electric motors exposed to the pressure existing at the high-pressure side of the turbo pump; electrical current is limited, while accelerating the rotor, by use of a 3-phase variac. Bearings for both the rotor and the motors are loose-radial-fit ball bearings lubricated with G-300 versilube silicone grease; the pump-rotor bearings and the motor-field windings are water-cooled. At 5000 rpm, stress safety factors for all rotor components are equal to or greater than 2.4. Tests have been made using air at no-flow conditions and for rotor speeds up to 3300 rpm; both the experimental results and the theoretical predictions are given in Figure 21; the agreement is considered to be excellent. Values of pumping speed predicted for the case in

FIGURE 19

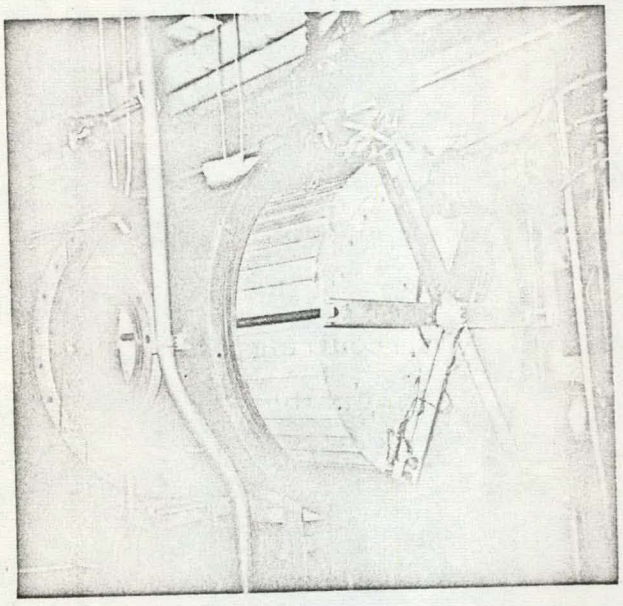

TURBO PUMP INSTALLED PARTLY IN VACUUM CHAMBER
(From Figure 16 of Ref. 41. Motor shown here has been replaced by two 5 horsepower motors)

FIGURE 20

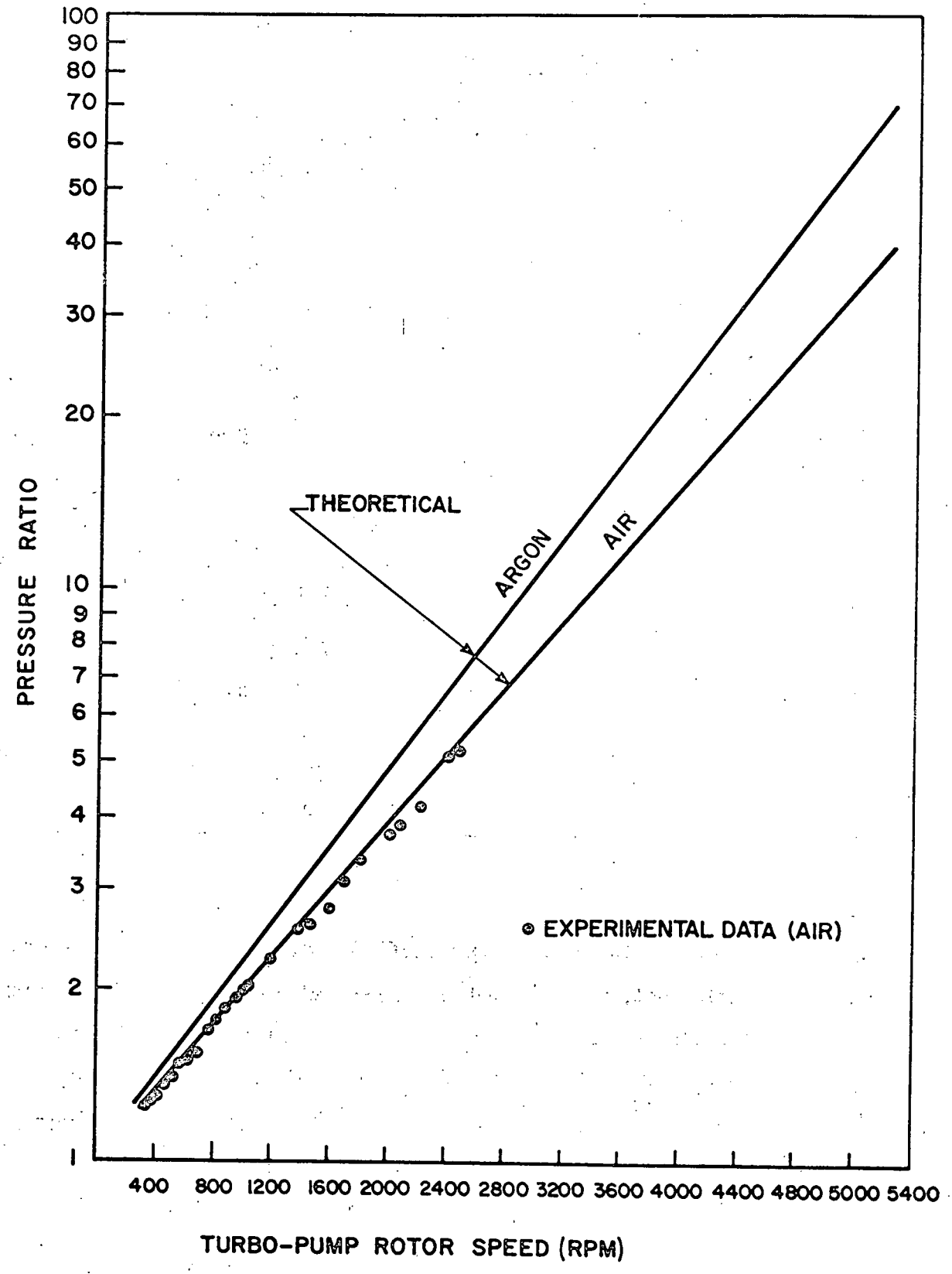


TURBO-PUMP PERFORMANCE AT ZERO FLOW
(Ref. 41, Figure 17)

FIGURE 21

TABLE VI

PRINCIPAL CHARACTERISTICS OF TURBO PUMP

| | First Stage | Second Stage |
|---|---|---|
| Rotor-Blade Angle | $20^{o}$ | $20^{o}$ |
| Stator-Blade Angle | $20^{o}$ | $10^{o}$ |
| Rotor-Blade Chord Length | 4.4 cm | 5.4 cm |
| Stator-Blade Chord Length | 5.1 cm | 6.0 cm |
| Number of Rotor Blades | 48 | 48 |
| Number of Stator Blades | 48 | 48 |
| Rotor Pumping Area | 1.37 $m^2$ | 1.60 $m^2$ |
| Rotor-Blade Speed at 5000 rpm | 190 m/sec | 222 m/se |

which the present turbo pump is used as a boost pump on the low-pressure side of an unbaffled 10-inch CVC Type PMC-4100 diffusion pump are given in Figure 22. Note that, if $10^{19}$ molecules/sec at $300^{o}$K are to be pumped, then the unbaffled 10-inch diffusion pump would pump at $8 \times 10^{-5}$ torr whereas the combined pumps, with the rotor turning at 5000 rpm, would pump at $8 \times 10^{-6}$ torr. This performance would be adequate for the collimating-chamber pumping system.*

* See Note Added in Proofreading, p. iii.

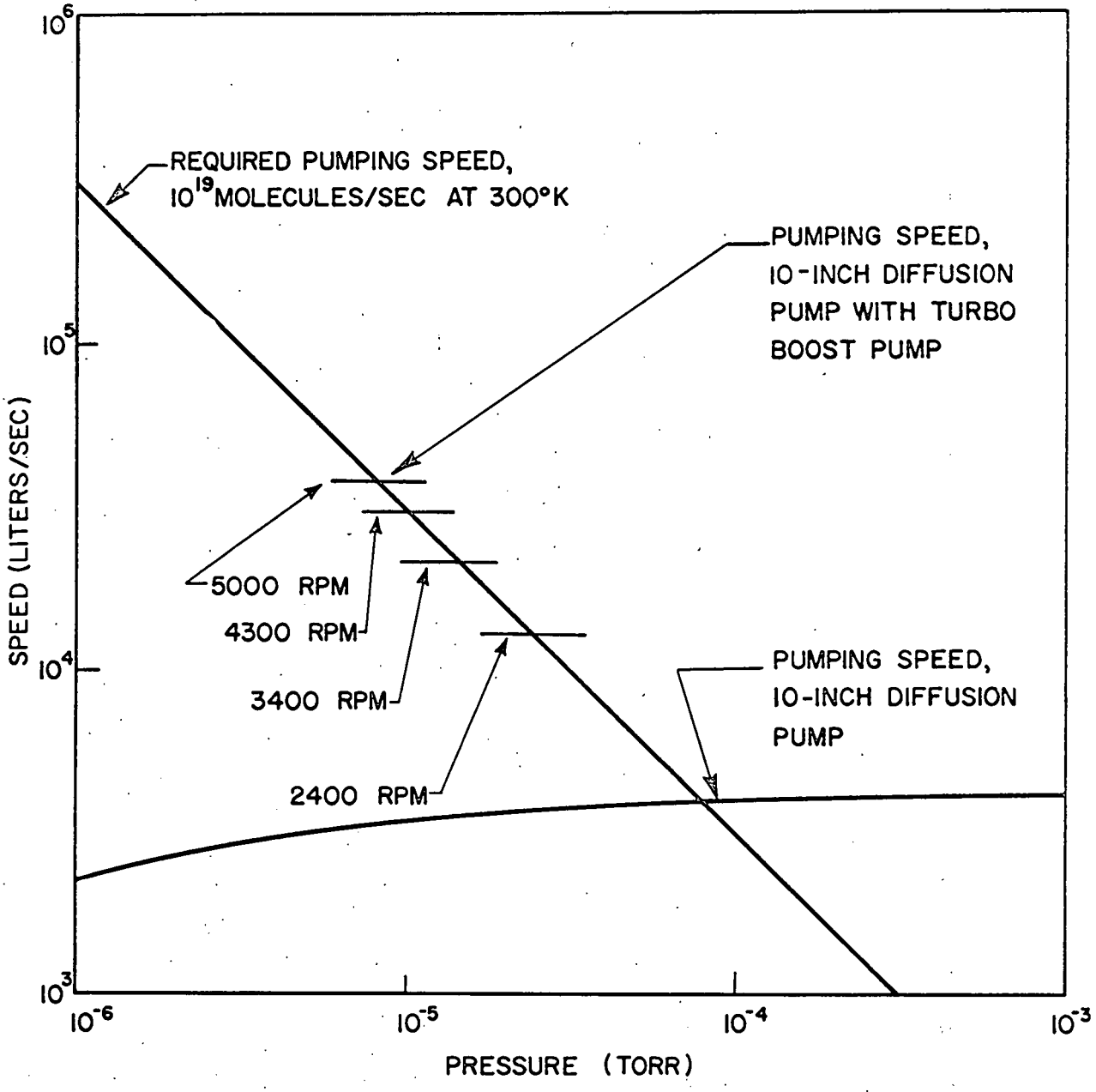


REQUIRED PUMPING SPEED AND CAPABILITY OF AN UNBAFFLED 10-INCH DIFFUSION PUMP WITH AND WITHOUT TURBO BOOST PUMP
(Ref. 41, Figure 12)

FIGURE 22

Consider finally the pumping system for the detecting chamber. As indicated in Table III, the detecting-chamber pumping system must remove (neglecting outgassing) $8.6 \times 10^{15}$ molecules/sec. At a chamber pressure of $10^{-6}$ torr, beam attenuation due to background scattering is approximately 1%, an acceptable value. A molecular flow rate of $8.6 \times 10^{15}$ molecules/sec at $10^{-6}$ torr and $300^{\circ}$K corresponds to a volume flow rate of 267 $\ell$/sec. A pumping capacity adequate for the sum of this flow rate and a typical outgassing rate is provided by a baffled 10-inch CVC Type PMC-4100 diffusion pump (1600 $\ell$/sec pumping speed at $10^{-6}$ torr).

## ANTICIPATED STUDIES

Preliminary studies using the heated beam will be on the performance of the beam. Measurements of the speed distribution (facilitated by use of the chopper-selector), intensity (facilitated by use of the quantitative detector calibration given in Figure 14) and degree of ionization (facilitated by use of a deflecting electrostatic field crossing the beam) would be useful when comparing realized performance with predicted performance, when comparing the performance of this beam with the performances of contemporary beams (e.g., References 9-29) and when interpreting collision data obtained with this beam.

These measurements of beam performance are to be followed by measurements of scattering and accommodation of argon by engineering surfaces. The scattering measurements would extend previous scattering measurements in that they would be made at higher energies - at energies up to several electron volts (See, e.g., References 1-3 and 78 for references to earlier scattering experiments, References 79-89 for descriptions of more recent scattering experiments and Reference 90 for an informal discussion of prospects and future developments in applications of molecular beams.) The accommodation measurements would be among the first accommodation measurements made using a molecular beam. (See, e.g., Reference 91 for a survey of the status of accommodation measurements in 1961 and References 83, 84, 85 and 87 for descriptions of molecular-beam measurements of accommodation.) Measurements at large incidence angles (with incidence angles measured relative to the normal to the surface)

are to be included; available data indicate that the probability of specular reflection is greatest at large incidence angles; studies of collisions at these incidence angles must be included in studies of drag and heating of space vehicles and satellites.

In a concurrent study, attempts will be made to measure the sitting times of molecules on cooled targets. The time of arrival of a burst of molecules at the target can be computed if the time of departure from the chopper-selector, the distance from the chopper-selector to the target, and the speed of the burst are known; values of the first two parameters can be measured directly whereas the value of the third parameter can be computed from measured values of chopper-selector parameters. The time of departure of the burst of molecules from the target can be computed if the time of arrival at a detector, the distance from the target to the detector, and the speed of the burst are known; values of the first two parameters can be measured directly whereas the value of the third parameter can be computed from measurements of the distance and time of flight between two detectors mounted in series in the path of departing molecules.

Future studies might include studies of molecule-molecule collisions at energies above 1 ev, using either crossed beams or a single beam and a gaseous target. Many chemical reactions involve energies of several electron volts. (See, e.g., References 3, 92 and 93 for reviews of molecular-beam studies of molecule-molecule collisions and References 85 and 94-99 for descriptions of recent molecular-beam studies of gas-phase chemical reactions.)

One might consider also studies of chemical reactions involving solid surfaces (e.g., References 3, 85 and 100). Preparing and maintaining a surface of known state would be even more important for such studies than for studies of scattering and accommodation. The rate of sorption, by the surface, of molecules from the residual gas in the detecting chamber would have to be reduced, perhaps by reducing the residual-gas density. Reducing the residual-gas density might require both a reduction in rate of outgassing from the chamber walls and augmentation of the speed of the detecting-chamber pumping system.

THIS PAGE

WAS INTENTIONALLY

LEFT BLANK

## REFERENCES


1. Smith, K.F., Molecular Beams. London: Methuen and Co., Ltd., 1955.
2. Ramsey, N.F., Molecular Beams. London: Oxford University Press, 1956.
3. Estermann, I., (Editor), Recent Research in Molecular Beams. New York: Academic Press, 1959.
4. Devienne, F.M., (Editor), Rarefied Gas Dynamics. London: Pergamon Press, 1960.
5. Miller, G.H., (Editor), Proceedings of the Atomic and Molecular Beams Conference. Denver: University of Denver, 1960.
6. Talbot, L., (Editor), Rarefied Gas Dynamics. New York: Academic Press, 1961.
7. Kantrowitz, A., and Grey, J., "A High Intensity Source for the Molecular Beam: Part I, Theoretical", Rev. Sci. Inst. 22: 328-332, May 1951.
8. Kistiakowsky, G.B., and Slichter, W.P., "A High Intensity Source for the Molecular Beam: Part II, Experimental", Rev. Sci. Inst. 22: 333-337, May 1951.
9. Becker E.W., and Bier, K., "Die Erzeugung eines intensiven, teilweise monochromatisierten Wasserstoff-Molekularstrahles mit einer Laval-Düse", Z. für Naturforschung 9a: 975-986, November 1954.
10. Becker, E.W., and Henkes, W., "Geschwindigkeitsanalyse von Laval-Strahlen", Z. für Physik 146: 320-332, 1956.
11. Becker, E.W., Bier, K., and Henkes, W., "Strahlen aus kondensierten Atomen und Molekeln im Hochvakuum", Z. für Physik 146: 333-338, 1956.
12. Hagena, O., and Henkes, W., "Untersuchung der thermischen Relaxation bei Düsenströmungen durch Analyse der gaskinetischen Geschwindigkeitsverteilung", Z. für Naturforschung 15a: 851-859, October 1960.
13. Becker, E.W., Klingelhöfer, R., and Lohse, P., "Strahlen aus kondensiertem Helium im Hochvakuum", Z. für Naturforschung 16a: 1259, 1961.
14. Bier, K., and Schmidt, B., "Zur Form der Verdichtungsstösse in frei expandierenden Gasstrahlen", Z. für angewandte Physik 13: 493-500, November 1961.
15. Parker, H.M., Kuhlthau, A.R., Zapata, R., and Scott, J.E., Jr., "The Application of Supersonic Beam Sources to Low-Density, High-Velocity Experimentation", published in Reference 4.
16. Zapata, R.N., and Parker, H.M., "Experimental Analysis of Molecular Beams at High Source Pressures", published in Reference 5.

17. Zapata, R.N., Parker, H.M., and Bodine, J.H., "Performance of a Supersonic Molecular Beam", published in Reference 6.

18. Scott, J.E., Jr., and Kuhlthau, A.R., "Laboratory Investigation of the Basic Nature of Low Density Gas Flow at High Speeds. Annual Progress Report for the Period 1 January 1961 to 31 December 1961", Report No. AST-4435-116-62U. Charlottesville, Virginia: Research Laboratorie for the Engineering Sciences, University of Virginia, February 1962.

19. Skinner, G.T., "Molecular Beam for the Study of High-Temperature-Gas Collison Processes", Physics of Fluids 4: 1172-1176, September 1961.

20. Drake, R.M. Jr., and Deckers, J., "High Energy Molecular Beam Research. First Annual Progress Report, 1 August 1959 - 1 August 1960", Report No. ME-FLD-2. Princeton: Mechanical Engineering Dept., Princeton University, 31 August 1960.

21. Deckers, J., and Fenn, J.B., "A High Intensity Molecular Beam Apparatus". Princeton: School of Engineering, Princeton University, 15 June 1962.

22. Fenn, J.B., and Deckers, J., "Molecular Beams from Nozzle Sources". Princeton: School of Engineering, Princeton University, 27 June 1962.

23. Devienne, F.M., and Souquet, J., "Production of a Molecular Beam at a Very High Speed and Relatively Great Density; Development of a Molecular Gun", published in Reference 6.

24. Oman, R.A., "Analysis of a Skimmer for a High-Intensity Molecular Beam Using a Three-Fluid Model", Research Dept. Memorandum RM-214. Bethpage, New York: Grumman Aircraft Engineering Corp. October 1962.

25. Oman, R.A., Weiser, C.H., and Calia, V.S., "Interaction of High-Energy Gas Molecules with Solid Surfaces - Status Report No. 1", Research Dept. Memorandum RM-215. Bethpage, New York: Grumman Aircraft Engineering Corp., October 1962.

26. Patterson, G.N., et al, Annual Progress Report 1962. Toronto: University of Toronto Institute of Aerophysics, October 1962. Also French, B., "The Surface Interaction Program at UTIA", presented at Conference on Molecular and Atomic Gas Beams and Related Problems (no proceedings available). Charlottesville: University of Virginia, 13-14 May 1963.

27. Sherman, F.S., Personal Communication, 27 November 1962; Talbot, L., Personal Communication, 26 March 1963; and Schaaf, S.A. Personal Communication, 14 June 1963.

28. Fristrom, R., "Projected Molecular Beam Research at APL", presente at Conference on Molecular and Atomic Gas Beams and Related Problem (no proceedings available). Charlottesville: University of Virginia, 13-14 May 1963.

29. McGinn, J., and Wachman, H., "Status of a New High Intensity Molecular Beam Apparatus at the Space Sciences Laboratory", presented at Conference on Molecular and Atomic Gas Beams and Related Problems (no proceedings available). Charlottesville: University of Virginia, 13-14 May 1963.

30. Zacharias, J.R., and Haun, R.D. Jr., "Well-Collimated Atomic Oven Beams", Quarterly Progress Report No. 35, pp. 34-37. Cambridge: Mass. Institute of Technology, Research Laboratory of Electronics, 15 October 1954.

31. Datz, S., Minturn, R.E., and Taylor, E.H., "Multiple Aperture Slits for Molecular Beam Sources", Rev. Sci. Inst. 32: 210, February 1961.

32. Fite, W.L., "Some Applications of Modulated Atomic Beam Experimentation", published in Reference 5.

33. Brackmann, R.T., and Fite, W.L., "Condensation of Atomic and Molecular Hydrogen at Low Temperatures", J. Chem. Phys. 34: 1572-1579, May 1961.

34. Kuluva, N.M., and Knuth, E.L., "Sorption Pumping at Pressures Less Than $10^{-5}$ Torr", 1962 Transactions of the Ninth National Vacuum Symposium of the American Vacuum Society, 237-242. New York: The MacMillan Co., 1962.

35. Henry, R.J., "Design of a High-Speed, High-Intensity Molecular Beam", Dept. of Engineering, M.S. Thesis. Los Angeles: University of California at Los Angeles, June 1961.

36. Callinan, J.P., "A Method for Determining the Velocity Distribution in a Reflected Molecular Beam", Dept. of Engineering, M.S. Thesis. Los Angeles: University of California at Los Angeles, June 1961.

37. Plue, R.L., "A Velocity Selector for High-Speed Molecular Beams", Dept. of Engineering, M.S. Thesis. Los Angeles: University of California at Los Angeles, June 1962.

38. Johnston, G.L., "Some Problems of Non-Equilibrium Ionized Gas Flows", Dept. of Engineering, M.S. Thesis. Los Angeles: University of California at Los Angeles, June 1962.

39. Kuluva, N.M., "Vacuum Pumping by Adsorption", Dept. of Engineering, M.S. Thesis. Los Angeles: University of California at Los Angeles, June 1962.

40. Barnes, J.W., Jr., "Design of a Low-Density, Hypervelocity Argon Nozzle-Diffuser for Application to a High-Intensity Molecular Beam", Dept. of Engineering, M.S. Thesis. Los Angeles: University of California at Los Angeles, January 1963.

41. Iacobellis, S.F., "Analytical and Experimental Study of a Novel Turbomolecular Vacuum Pump", Dept. of Engineering, M.S. Thesis. Los Angeles: University of California at Los Angeles, June 1963.

42. Quan, D., "Analysis and Calibration of a Molecular Beam Detector", Dept. of Engineering, M.S. Thesis. Los Angeles: University of California at Los Angeles, June 1963.

43. Liepmann, H.W., and Roshko, A., Elements of Gasdynamics. New York: John Wiley and Sons, Inc., 1960.

44. Owen, P.L., and Thornhill, C.K., "The Flow in an Axially-Symmetric Supersonic Jet From a Nearly-Sonic Orifice into a Vacuum", Gr. Britain ARC Technical Report R&M No. 2616, 1952.

45. Love, E.S., Grigsby, C.E., Lee, L.P., and Woodling, M.J., "Experimental and Theoretical Studies of Axisymmetric Free Jets", NASA TR R-6, 1959.

46. Eastman, D.W., and Radtke, L.P., "Location of the Normal Shock Wave in the Exhaust Plume of a Jet", AIAA Journal 1: 918-919, April 1963.

47. Sherman, F.S., "Self-Similar Development of Inviscid Hypersonic Free-Jet Flows", Technical Report Fluid Mechanics 6-90-63-61. Sunnyvale, California: Lockheed Missiles and Space Co., 23 May 1963.

48. Wilcox, D.E., Weir, A., Jr., Nicholls, J.A., and Dunlap, R., "Location of Mach Discs and Diamonds in Supersonic Air Jets", J. Aero. Sciences 24: 150-152, February 1957.

49. Reis, V.H., "Free Expansion of Pure and Mixed Gases from Small Sonic Nozzles", Mechanical Engineering Dept. Report No. FLD-7. Princeton: Princeton University, May 1962.

50. Muckenfuss, C., "Mean-Free-Path Concept in Gas Dynamics", Physics of Fluids 5: 165-168, February 1962.

51. Troitskii, V.S., "The-Mean-Free-Path of Molecules in a Molecular Beam", Soviet Physics JETP 14: 281, February 1962.

52. Bennett, A.I., "Distribution of Velocities in Molecular Beams of Potassium", Dept. of Physics, Ph.D. Thesis. Pittsburgh: Carnegie Institute of Technology, May 1953.

53. McFee, J.H., and Marcus, P.M., "Velocity Distributions in Direct and Reflected Molecular Beams", Technical Report No. 1, Contract Nonr-760(11) NR 019-602. Pittsburgh: Carnegie Institute of Technology, January 1960.

54. Eldridge, J.A., "Experimental Test of Maxwell's Distribution Law", Phys. Rev. 30: 931-935, December 1927.

55. Hubert, P., Joly, R., and Signarbieux, C.L., "Mechanical Velocity Selector for Filtering Higher Order Reflections", The International Conference on the Neutron Interactions with the Nucleus, held at Columbia University, September 9-13, 1957. Oak Ridge: U.S. Atomic Energy Commission, 1957.

56. Hostettler, H.U., and Bernstein, R.B., "Improved Slotted Disk Type Velocity Selector for Molecular Beams", Rev. Sci. Inst. 31: 872-877, May 1960.

57. Davis, H.J., and Bodine, J.H., "Preliminary Design of a Multi-Disk Velocity Selector", Report No. AST-4435-107-60U. Charlottesville: University of Virginia, September 1960.

58. Miller, R.C., and Kusch, P., "Velocity Distributions in Potassium and Thallium Atomic Beams", Phys. Rev. 99: 1314-1321, August 15, 1955.

59. Holt, N., "High Transmission Mechanical Neutron-Monochromator for Filtering Higher Order Reflections", Rev. Sci. Inst. 28: 1-3, January 1957.

60. Dash, J.G., and Sommers, H.S., "A High Transmission Slow Neutron Velocity Selector", Rev. Sci. Inst. 24: 91-96, February 1953.

61. Wessel, G., and Lew, H., "Hyperfine Structures of Silver and Gold by the Atomic Beam Magnetic Resonance Method", Phys. Rev. 92: 641-646, November 1, 1953.

62. Fricke, G., "Ein universeller Detektor für Molekularstrahlen", Z. für Physik 141: 166-170, April 1955.

63. Bernhard, F., "Ein neues lichtstarkes Massenspektrometer zum Nachweis von Atom-bzw. Molekularstrahlen", Z. für angewandte Physik 9: 68-73, February 1957.

64. Friedmann, H., "Ein beweglicher Universaldetektor für Atomstrahlen", Z. für Physik 156: 598-602, October 1959.

65. Weiss, R., "Molecular Beam Electron Bombardment Detector", Rev. Sci. Inst. 32: 397-401, April 1961.

66. Bennewitz, H.G., and Wedemeyer, R., "Ein Molekularstrahldetektor mit Electronenstossionisierung und Vierpol-Massenfilter", Z. für Physik 172: 1-18, January 1963.

67. Arnot, F.L., Collision Processes in Gases. London: Methuen & Co., Ltd., 1950.

68. Lopez-Gonzales, J. de Dios, Carpenter, F.G., and Deitz, V.R., "Adsorption of Nitrogen and Argon on Mineralogical Graphite and Diamond at 77 and 90°K", J. of Phys. Chem. 65: 1112-1119, July 1961.

69. Garden, L.A., Kington, G.L., and Laing, W., "The Heats of Sorption, Isotherms, and Entropies of Argon in Natural and Calcium Chabazites", Faraday Society Transactions 51: 1558-1569, November 1955.

70. Beher, J.T., "Adsorbents in Liquid Oxygen Containers", Proceedings of the 1956 Cryogenic Engineering Conference 182-187. Boulder: University of Colorado, 1957.

71. Gibson, G., Jordan, W.C., Lauer, E.J., and Ullman, J.R. "A Liquid Helium-Cooled Trap for Pumping Gas by Adsorption", UCRL-6113. Livermore: Lawrence Radiation Laboratory, October 1960.

72. Feinleib, M., "New Approaches to Sorption Pumping", presented at Conference on Physical Electronics, Mass. Institute of Technology, March 31, 1961.

73. Becker, W., "Uber eine neue Molekularpumpe", Proceedings of the Fir International Congress on Vacuum Technology, 10-13 June 1958, Namur, Belgium. London: Pergamon Press, 1960.

74. Hablanian, M., "The Axial Flow Compressor as a High Vacuum Pump", Proceedings of the First International Congress on Vacuum Technology, 10-13 June 1958, Namur, Belgium. London: Pergamon Press, 1960.

75. Kruger, C.H., "The Axial-Flow Compressor in the Free-Molecule Rang Dept. of Mechanical Engineering, Ph.D. Thesis. Cambridge: Mass. Institute of Technology, February 1960.

76. Kruger, C.H., and Shapiro, A.H., "The Axial-Flow Compressor in the Free-Molecule Range", published in Reference 6.

77. Maulbetsch, J.S., and Shapiro, A.H., "Free-Molecule Flow in the Axia Flow Turbo-Vacuum Pump", Fluid Mechanics Laboratory Publication No. 63-3. Cambridge: Dept. of Mechanical Engineering, Mass. Institut of Technology, March 1963.

78. Estermann, I., "Molecular Beam Technique", Rev. of Modern Physics 18: 300-323, July 1946.

79. Hurlbut, F.C., "An Experimental Molecular Beam Investigation of the Scattering of Molecules from Surfaces", Report No. HE-150-118. Berkeley: Institute of Engineering Research, University of California, December 1, 1953.

80. Merlic, E., "An Experimental Determination of Reflection Coefficients for Air on Aluminum", Report No. HE-150-141. Berkeley: Institute of Engineering Research, University of California, August 31, 1956.

81. Hurlbut, F.C., "Studies of Molecular Scattering at the Solid Surface", J. of Appl. Physics 28: 844-850, August 1957.

82. Hurlbut, F.C., and Beck, D.E., "New Studies of Molecular Scattering at the Solid Surface", Report No. HE-150-166. Berkeley: Institute of Engineering Research, University of California, August 11, 1959.

83. Holister, G.S., Brackman, R.T., and Fite, W.L., "The Use of Modula Atomic-Beam Techniques for the Study of Space-Flight Problems", Report GA-1024. San Diego: General Atomic Division of General Dynamics Corp., October 14, 1959.

84. McFee, J.H., and Marcus, P.M., "Velocity Distributions in Direct and Reflected Atomic Beams", Technical Report No. 1. Pittsburgh: Carneg Institute of Technology, Dept. of Physics. January 8, 1960.

85. Fite, W.L., "Some Applications of Modulated Atomic Beam Experimentation", published in Reference 5.

86. Hurlbut, F.C., "Recent Studies of Particle Surface Interactions", published in Reference 5.

87. McFee, J.H., and Marcus, P.M., "Molecular Beam Investigation of Energy Exchange Between a Gas and a Solid Surface", published in Reference 5.

88. Brackmann, R.T., and Fite, W.L., "Condensation of Atomic and Molecular Hydrogen at Low Temperatures", J. Chem. Phys. 34: 1572-1579, May 1961.

89. Crews, J.C., "Scattering of Helium and Argon from the Cleavage Plane of Lithium Fluoride", J. Chem. Phys. 37: 2004-2008, November 1, 1962.

90. Smolderen, J.J., (Editor), Proceedings of the Meeting on Molecular Beam Techniques, 1 July 1962, Nice, France. Rhode-Saint-Genese, Belgium: Training Center for Experimental Aerodynamics, March 1963.

91. Wachman, H.Y., "The Thermal Accommodation Coefficient: A Critical Survey", ARS Journal 32: 2-12, January 1962.

92. Schlier, C., "Neuere Messungen mit Hilfe der Molekularstrahltechnik", Fortschritte der Physik 5: 378-420, 1957.

93. Pauly, H., "Streuversuche an Molekularstrahlen und Zwischenmolekulare Kräfte", Fortschritte der Physik 9: 613-687, 1961.

94. Datz, S., "The Application of Molecular Beam Techniques to Chemically Reactive Collisions", published in Reference 5.

95. Kusch, P., "Studies Involving the Complexes of the Alkali Halides", published in Reference 5.

96. Herschbach, D.R., "Analysis of Reactive Scattering in Crossed Molecular Beams", J. Chem. Phys. 33: 1870-1871, December 1960.

97. Herschbach, D.R., Kwei, G.H., and Norris, J.A., "Reactive Scattering in Crossed Molecular Beams. K Atoms with $CH_3I$ and $C_2H_5I$", J. Chem. Phys. 34: 1842-1843, May 1961.

98. Ross, J., and Greene, E.F., "The Study of Chemical Reactions in Crossed Molecular Beams", presented at the XII International Solvay Conference, Brussels, November 1962.

99. Beck, D., Greene, E.F., and Ross, J., "Study of the Reaction of K with HBr in Crossed Molecular Beams", J. Chem. Phys. 37: 2895-2906, December 15, 1962.

100. Hoenig, S.A., "A Study of Oxygen Recombination on Metallic Surfaces by Means of an Atomic Beam", Report No. HE-150-173. Berkeley: Institute of Engineering Research, University of California, October 7, 1960.